Table 7. The top 5 canonical pathways associated with the 106 genes in which IFN response is suppressed by HCV infection.

Category	P value	Ratio	Associated genes
Interferon Signaling	4.41E-11	7/30 genes	IFIT1, IFIT3, IFNGR1, IRF1, MX1, STAT1, TAP1
Type I Diabetes Mellitus Signaling	1.08E-04	5/119 genes	HLA-E, IFNGR1, IRF1, RIPK1, STAT1
Antigen Presentation Pathway	5.29E-04	3/39 genes	HLA-E, TAP1, TAP2
Primary Immunodeficiency Signaling	1.64E-03	3/63 genes	BLNK, TAP1, TAP2
Activation of IRF by Cytosolic Pattern Recognition Receptors	2.95E-03	3/73 genes	ISG15, RIPK1, STAT1

doi:10.1371/journal.pone.0023856.t007

treatment in the presence of HCV infection, 7 genes in the IFN Signaling pathway became unresponsive (Table 6). Reduction in IFN responsiveness was also observed for *STAT1* (4.27 fold in the absence of HCV to 2.29 fold in the presence of HCV, $P = 4.04 \times 10^{-4}$), as well as 5 of 7 genes downstream of *STAT1* (*IFIT1*, *IFIT3*, *IRF1*, *MX1*, and *TAP1*). As shown in Figure 3, IFN

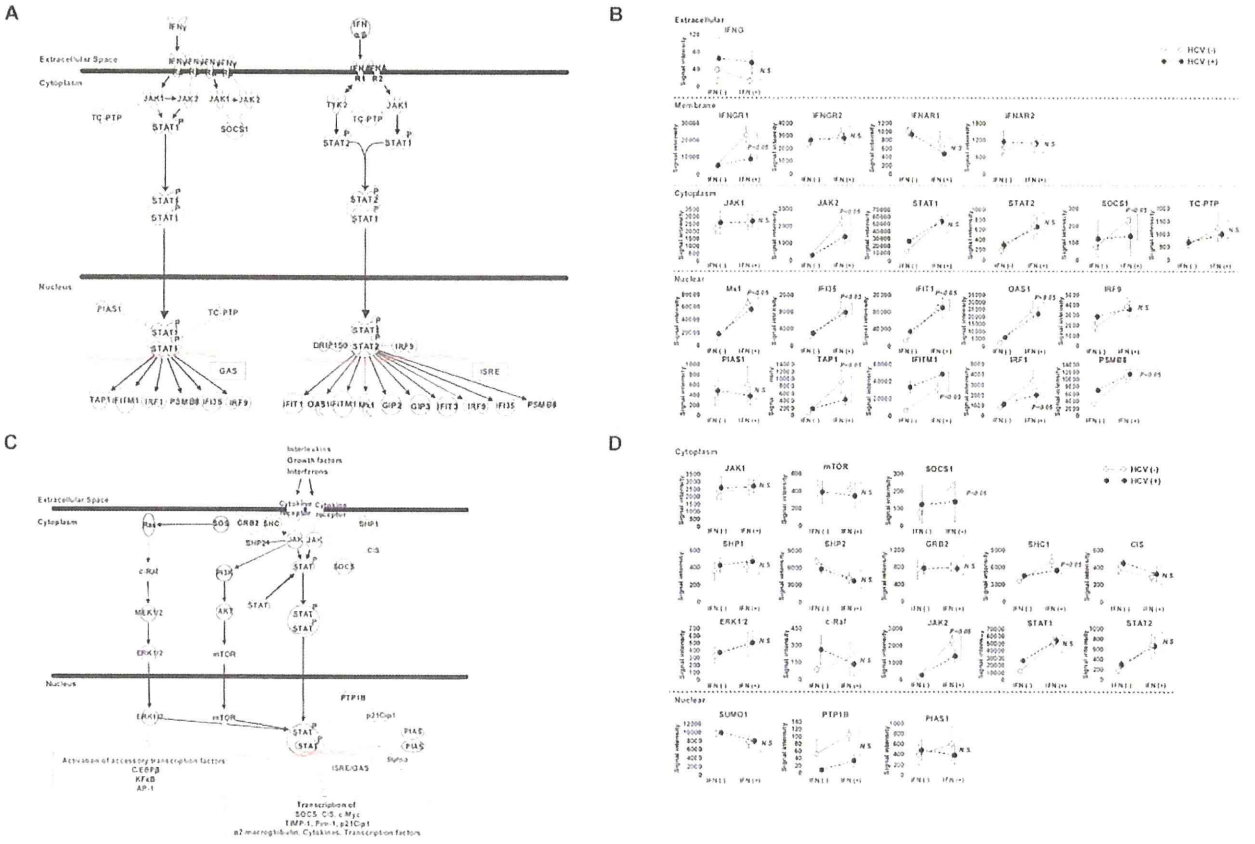

Figure 6. Changes in expression of genes in the IFN and JAK-STAT signaling pathways under HCV infection and/or IFN administration. A) An overview of the IFN signaling pathway consisting of 26 representative genes is shown. Genes illustrated as gray shapes were not included in this study. B) Relative expression levels of genes with/without HCV infection and/or IFN administration were plotted (closed dots: with HCV infection; open dots: without HCV infection) using microarray data. The slopes of the dashed and solid lines represent IFN responsiveness with and without HCV infection, respectively. In 21 of the 22 examined genes in the IFN signaling pathway, signal intensities increased and IFN responsiveness was repressed following HCV infection. Student's *t*-test was used for statistical analysis. C) An overview of the JAK-STAT signaling pathway consisting of 22 representative gene products is shown. Genes illustrated as gray shapes were not included in this study. D) Relative expression levels of genes with/without HCV infection and/or IFN administration were plotted using microarray data (closed dots: with HCV infection; open dots: without HCV infection). Signal intensities increased following HCV infection in 16 of 22 genes in the JAK-STAT signaling pathway, and IFN response was suppressed in 9 genes. Statistical analysis was performed using Student's *t*-test.
doi:10.1371/journal.pone.0023856.g006

Table 8. The 33 genes that remained more than 3-fold up-regulated following IFN treatment in HCV-infected mice.

ID	Symbol	Location	Type(s)
214995_s_at	APOBEC3F	unknown	enzyme
204205_at	APOBEC3G	Nucleus	enzyme
206011_at	CASP1	Cytoplasm	peptidase
204533_at	CXCL10	Extracellular Space	cytokine
210163_at	CXCL11	Extracellular Space	cytokine
203915_at	CXCL9	Extracellular Space	cytokine
218943_s_at	DDX58	Cytoplasm	enzyme
231577_s_at	GBP1 (includes EG:2633)	Cytoplasm	enzyme
235175_at	GBP4 (includes EG:115361)	Cytoplasm	enzyme
225710_at	GNB4	Plasma Membrane	enzyme
1553646_at	HDX	unknown	other
213069_at	HEG1	unknown	other
206332_s_at	IFI16	Nucleus	transcription regulator
219209_at	IFIH1	Nucleus	enzyme
217502_at	IFIT2	unknown	other
204747_at	IFIT3	Cytoplasm	other
205992_s_at	IL15	Extracellular Space	cytokine
204698_at	ISG20	Nucleus	enzyme
205841_at	JAK2	Cytoplasm	kinase
210302_s_at	MAB21L2	unknown	other
223298_s_at	NT5C3	Cytoplasm	phosphatase
205660_at	OASL	unknown	enzyme
205801_s_at	RASGRP3	Cytoplasm	other
242625_at	RSAD2	unknown	enzyme
228531_at	SAMD9	unknown	other
230036_at	SAMD9L	unknown	other
219885_at	SLFN12	Nucleus	enzyme
206271_at	TLR3	Plasma Membrane	transmembrane receptor
214329_x_at	TNFSF10	Extracellular Space	cytokine
221371_at	TNFSF18	Extracellular Space	cytokine
203610_s_at	TRIM38	unknown	other
219211_at	USP18	Cytoplasm	peptidase
200629_at	WARS	Cytoplasm	enzyme

doi:10.1371/journal.pone.0023856.t008

signaling was activated in the presence of HCV, and the expression of *STAT1* was more than 3.0 fold up-regulated by HCV infection (data not shown). *STAT1* expression was highest in mice with both HCV infection and IFN treatment, but downstream genes such as *MX1*, *IFIT1* and *IFIT3* showed reduced IFN response. Sarasin-Filipowicz et al. reported that IFN-induced *STAT1* phosphorylation was stronger in rapid responders than in non-rapid responders [61]. Reduced induction of genes downstream of *STAT1* by IFN under HCV infection might reflect reduced phosphorylation of *STAT1*, although we did not quantify *STAT1* phosphorylation in this study.

Recently, an *IL-28B* genetic polymorphism strongly associated with response to IFN-α plus ribavirin combination therapy [12], as well as with hepatic ISG expression [62], was identified. Further studies using chimeric mice transplanted with hepatocytes carrying different genotypes of candidate genes such as *IL-28B* will be important in order to elucidate possible mechanisms underlying host-specific responses.

In conclusion, we performed cDNA microarray analysis using HCV-infected human hepatocyte chimeric mice, which allowed us to analyze the direct effects of IFN treatment and HCV infection without the confounding effects of the lymphocytic immunological response. These results might provide molecular insights into possible mechanisms used by HCV to evade IFN-induced immune responses, as well as suggest novel therapeutic targets and a potential new indication for interferon therapy. Further analysis of the genes identified in our study would be worthwhile in order to improve efficacy of the therapy for chronic hepatitis C.

Acknowledgments

This study was carried out at the Research Center for Molecular Medicine, Faculty of Medicine, Hiroshima University and the Analysis Center of Life Science, Hiroshima University. The authors thank Rie Akiyama and Ruri Mikami for their excellent technical assistance, and Aya Furukawa for clerical assistance.

Author Contributions

Conceived and designed the experiments: MT YF NH MI ST KC. Performed the experiments: MT YF NH FM TT. Analyzed the data: MT YF YZ MO TK HA DM. Contributed reagents/materials/analysis tools: MT NH MI FM TT KC. Wrote the paper: MT YF ST HO CNH KC.

References

1. Alter HJ, Purcell RH, Shih JW, Melpolder JC, Houghton M, et al. (1989) Detection of antibody to hepatitis C virus in prospectively followed transfusion recipients with acute and chronic non-A, non-B hepatitis. N Engl J Med 321: 1494–1500.
2. Cooper S, Erickson AL, Adams EJ, Kansopon J, Weiner AJ, et al. (1999) Analysis of a successful immune response against hepatitis C virus. Immunity 10: 439–449.
3. Lee SH, Kim YK, Kim CS, Seol SK, Kim J, et al. (2005) E2 of hepatitis C virus inhibits apoptosis. J Immunol 175: 8226–8235.
4. Fried MW, Shiffman ML, Reddy KR, Smith C, Marinos G, et al. (2002) Peginterferon alfa-2a plus ribavirin for chronic hepatitis C virus infection. N Engl J Med 347: 975–982.
5. Hoofnagle JH, Ghany MG, Kleiner DE, Doo E, Heller T, et al. (2003) Maintenance therapy with ribavirin in patients with chronic hepatitis C who fail to respond to combination therapy with interferon alfa and ribavirin. Hepatology 38: 66–74.
6. Manns MP, McHutchison JG, Gordon SC, Rustgi VK, Shiffman M, et al. (2001) Peginterferon alfa-2b plus ribavirin compared with interferon alfa-2b plus ribavirin for initial treatment of chronic hepatitis C: a randomised trial. Lancet 358: 958–965.
7. Abbate I, Lo Iacono O, Di Stefano R, Cappiello G, Girardi E, et al. (2004) HVR-1 quasispecies modifications occur early and are correlated to initial but not sustained response in HCV-infected patients treated with pegylated- or standard-interferon and ribavirin. J Hepatol 40: 831–836.
8. Akuta N, Suzuki F, Kawamura Y, Yatsuji H, Sezaki H, et al. (2007) Prediction of response to pegylated interferon and ribavirin in hepatitis C by polymorphisms in the viral core protein and very early dynamics of viremia. Intervirology 50: 361–368.
9. Akuta N, Suzuki F, Sezaki H, Suzuki Y, Hosaka T, et al. (2005) Association of amino acid substitution pattern in core protein of hepatitis C virus genotype 1b high viral load and non-virological response to interferon-ribavirin combination therapy. Intervirology 48: 372–380.
10. Conjeevaram HS, Fried MW, Jeffers LJ, Terrault NA, Wiley-Lucas TE, et al. (2006) Peginterferon and ribavirin treatment in African American and Caucasian American patients with hepatitis C genotype 1. Gastroenterology 131: 470–477.
11. Enomoto N, Sakuma I, Asahina Y, Kurosaki M, Murakami T, et al. (1996) Mutations in the nonstructural protein 5A gene and response to interferon in patients with chronic hepatitis C virus 1b infection. N Engl J Med 334: 77–81.
12. Ge D, Fellay J, Thompson AJ, Simon JS, Shianna KV, et al. (2009) Genetic variation in IL28B predicts hepatitis C treatment-induced viral clearance. Nature 461: 399–401.
13. Kitamura S, Tsuge M, Hatakeyama T, Abe H, Imamura M, et al. (2010) Amino acid substitutions in core and NS5A regions of the HCV genome can predict virological decrease with pegylated interferon plus ribavirin therapy. Antivir Ther 15: 1087–1097.
14. Sezaki H, Suzuki F, Kawamura Y, Yatsuji H, Hosaka T, et al. (2008) Poor Response to Pegylated Interferon and Ribavirin in Older Women Infected with Hepatitis C Virus of Genotype 1b in High Viral Loads. Dig Dis Sci.
15. Tanaka Y, Nishida N, Sugiyama M, Kurosaki M, Matsuura K, et al. (2009) Genome-wide association of IL28B with response to pegylated interferon-alpha and ribavirin therapy for chronic hepatitis C. Nat Genet 41: 1105–1109.
16. Kawai T, Takahashi K, Sato S, Coban C, Kumar H, et al. (2005) IPS-1, an adaptor triggering RIG-I- and Mda5-mediated type I interferon induction. Nat Immunol 6: 981–988.
17. Seth RB, Sun L, Ea CK, Chen ZJ (2005) Identification and characterization of MAVS, a mitochondrial antiviral signaling protein that activates NF-kappaB and IRF 3. Cell 122: 669–682.
18. Xu LG, Wang YY, Han KJ, Li LY, Zhai Z, et al. (2005) VISA is an adapter protein required for virus-triggered IFN-beta signaling. Mol Cell 19: 727–740.
19. Li XD, Sun L, Seth RB, Pineda G, Chen ZJ (2005) Hepatitis C virus protease NS3/4A cleaves mitochondrial antiviral signaling protein off the mitochondria to evade innate immunity. Proc Natl Acad Sci U S A 102: 17717–17722.
20. Abe T, Kaname Y, Hamamoto I, Tsuda Y, Wen X, et al. (2007) Hepatitis C virus nonstructural protein 5A modulates the toll-like receptor-MyD88-dependent signaling pathway in macrophage cell lines. J Virol 81: 8953–8966.
21. Moriishi K, Mochizuki R, Moriya K, Miyamoto H, Mori Y, et al. (2007) Critical role of PA28gamma in hepatitis C virus-associated steatogenesis and hepatocarcinogenesis. Proc Natl Acad Sci U S A 104: 1661–1666.
22. Moriishi K, Okabayashi T, Nakai K, Moriya K, Koike K, et al. (2003) Proteasome activator PA28gamma-dependent nuclear retention and degradation of hepatitis C virus core protein. J Virol 77: 10237–10249.
23. Moriya K, Fujie H, Shintani Y, Yotsuyanagi H, Tsutsumi T, et al. (1998) The core protein of hepatitis C virus induces hepatocellular carcinoma in transgenic mice. Nat Med 4: 1065–1067.
24. Moriya K, Nakagawa K, Santa T, Shintani Y, Fujie H, et al. (2001) Oxidative stress in the absence of inflammation in a mouse model for hepatitis C virus-associated hepatocarcinogenesis. Cancer Res 61: 4365–4370.
25. Moriya K, Yotsuyanagi H, Shintani Y, Fujie H, Ishibashi K, et al. (1997) Hepatitis C virus core protein induces hepatic steatosis in transgenic mice. J Gen Virol 78(Pt 7): 1527–1531.
26. Tanaka N, Moriya K, Kiyosawa K, Koike K, Gonzalez FJ, et al. (2008) PPARalpha activation is essential for HCV core protein-induced hepatic steatosis and hepatocellular carcinoma in mice. J Clin Invest 118: 683–694.
27. Mercer DF, Schiller DE, Elliott JF, Douglas DN, Hao C, et al. (2001) Hepatitis C virus replication in mice with chimeric human livers. Nat Med 7: 927–933.
28. Tateno C, Yoshizane Y, Saito N, Kataoka M, Utoh R, et al. (2004) Near completely humanized liver in mice shows human-type metabolic responses to drugs. Am J Pathol 165: 901–912.
29. Hiraga N, Imamura M, Tsuge M, Noguchi C, Takahashi S, et al. (2007) Infection of human hepatocyte chimeric mouse with genetically engineered hepatitis C virus and its susceptibility to interferon. FEBS Lett 581: 1983–1987.
30. Kimura T, Imamura M, Hiraga N, Hatakeyama T, Miki D, et al. (2008) Establishment of an infectious genotype 1b hepatitis C virus clone in human hepatocyte chimeric mice. J Gen Virol 89: 2108–2113.
31. Tsuge M, Hiraga N, Takaishi H, Noguchi C, Oga H, et al. (2005) Infection of human hepatocyte chimeric mouse with genetically engineered hepatitis B virus. Hepatology 42: 1046–1054.
32. Bolstad BM, Irizarry RA, Astrand M, Speed TP (2003) A comparison of normalization methods for high density oligonucleotide array data based on variance and bias. Bioinformatics 19: 185–193.
33. Irizarry RA, Hobbs B, Collin F, Beazer-Barclay YD, Antonellis KJ, et al. (2003) Exploration, normalization, and summaries of high density oligonucleotide array probe level data. Biostatistics 4: 249–264.
34. Joyce MA, Walters KA, Lamb SE, Yeh MM, Zhu LF, et al. (2009) HCV induces oxidative and ER stress, and sensitizes infected cells to apoptosis in SCID/Alb-uPA mice. PLoS Pathog 5: e1000291.
35. Walters KA, Joyce MA, Thompson JC, Smith MW, Yeh MM, et al. (2006) Host-specific response to HCV infection in the chimeric SCID-beige/Alb-uPA mouse model: role of the innate antiviral immune response. PLoS Pathog 2: e59.
36. Feld JJ, Nanda S, Huang Y, Chen W, Cam M, et al. (2007) Hepatic gene expression during treatment with peginterferon and ribavirin: Identifying molecular pathways for treatment response. Hepatology 46: 1548–1563.
37. Lanford RE, Guerra B, Lee H, Chavez D, Brasky KM, et al. (2006) Genomic response to interferon-alpha in chimpanzees: implications of rapid downregulation for hepatitis C kinetics. Hepatology 43: 961–972.
38. Honda M, Yamashita T, Ueda T, Takatori H, Nishino R, et al. (2006) Different signaling pathways in the livers of patients with chronic hepatitis B or chronic hepatitis C. Hepatology 44: 1122–1138.
39. Caillot F, Derambure C, Bioulac-Sage P, Francois A, Scotte M, et al. (2009) Transient and etiology-related transcription regulation in cirrhosis prior to hepatocellular carcinoma occurrence. World J Gastroenterol 15: 300–309.
40. Caillot F, Hiron M, Goria O, Gueudin M, Francois A, et al. (2009) Novel serum markers of fibrosis progression for the follow-up of hepatitis C virus-infected patients. Am J Pathol 175: 46–53.
41. Toh PP, Li JJ, Yip GW, Lo SL, Guo CH, et al. (2010) Modulation of metallothionein isoforms is associated with collagen deposition in proliferating keloid fibroblasts in vitro. Exp Dermatol 19: 987–993.
42. Brassard DL, Grace MJ, Bordens RW (2002) Interferon-alpha as an immunotherapeutic protein. J Leukoc Biol 71: 565–581.
43. Clemens MJ, Elia A (1997) The double-stranded RNA-dependent protein kinase PKR: structure and function. J Interferon Cytokine Res 17: 503–524.
44. Dong B, Silverman RH (1995) 2-5A-dependent RNase molecules dimerize during activation by 2-5A. J Biol Chem 270: 4133–4137.
45. Platanias LC, Fish EN (1999) Signaling pathways activated by interferons. Exp Hematol 27: 1583–1592.
46. Samuel CE (2001) Antiviral actions of interferons. Clin Microbiol Rev 14: 778–809, table of contents.
47. Staeheli P, Pitossi F, Pavlovic J (1993) Mx proteins: GTPases with antiviral activity. Trends Cell Biol 3: 268–272.
48. Bishop KN, Holmes RK, Sheehy AM, Malim MH (2004) APOBEC-mediated editing of viral RNA. Science 305: 645.
49. Bonvin M, Achermann F, Greeve I, Stroka D, Keogh A, et al. (2006) Interferon-inducible expression of APOBEC3 editing enzymes in human hepatocytes and inhibition of hepatitis B virus replication. Hepatology 43: 1364–1374.
50. Lecossier D, Bouchonnet F, Clavel F, Hance AJ (2003) Hypermutation of HIV-1 DNA in the absence of the Vif protein. Science 300: 1112.
51. Mangeat B, Turelli P, Caron G, Friedli M, Perrin L, et al. (2003) Broad antiretroviral defence by human APOBEC3G through lethal editing of nascent reverse transcripts. Nature 424: 99–103.

52. Mariani R, Chen D, Schrofelbauer B, Navarro F, Konig R, et al. (2003) Species-specific exclusion of APOBEC3G from HIV-1 virions by Vif. Cell 114: 21–31.
53. Noguchi C, Hiraga N, Mori N, Tsuge M, Imamura M, et al. (2007) Dual effect of APOBEC3G on Hepatitis B virus. J Gen Virol 88: 432–440.
54. Noguchi C, Ishino H, Tsuge M, Fujimoto Y, Imamura M, et al. (2005) G to A hypermutation of hepatitis B virus. Hepatology 41: 626–633.
55. Rosler C, Kock J, Kann M, Malim MH, Blum HE, et al. (2005) APOBEC-mediated interference with hepadnavirus production. Hepatology 42: 301–309.
56. Suspene R, Sommer P, Henry M, Ferris S, Guetard D, et al. (2004) APOBEC3G is a single-stranded DNA cytidine deaminase and functions independently of HIV reverse transcriptase. Nucleic Acids Res 32: 2421–2429.
57. Zhang H, Yang B, Pomerantz RJ, Zhang C, Arunachalam SC, et al. (2003) The cytidine deaminase CEM15 induces hypermutation in newly synthesized HIV-1 DNA. Nature 424: 94–98.
58. Komohara Y, Yano H, Shichijo S, Shimotohno K, Itoh K, et al. (2006) High expression of APOBEC3G in patients infected with hepatitis C virus. J Mol Histol 37: 327–332.
59. Wasmuth HE, Lammert F, Zaldivar MM, Weiskirchen R, Hellerbrand C, et al. (2009) Antifibrotic effects of CXCL9 and its receptor CXCR3 in livers of mice and humans. Gastroenterology 137: 309–319, 319 e301-303.
60. Asselah T, Bieche I, Laurendeau I, Paradis V, Vidaud D, et al. (2005) Liver gene expression signature of mild fibrosis in patients with chronic hepatitis C. Gastroenterology 129: 2064–2075.
61. Sarasin-Filipowicz M, Oakeley EJ, Duong FH, Christen V, Terracciano L, et al. (2008) Interferon signaling and treatment outcome in chronic hepatitis C. Proc Natl Acad Sci U S A 105: 7034–7039.
62. Honda M, Sakai A, Yamashita T, Nakamoto Y, Mizukoshi E, et al. (2010) Hepatic ISG expression is associated with genetic variation in interleukin 28B and the outcome of IFN therapy for chronic hepatitis C. Gastroenterology 139: 499–509.

BRIEF REPORT

Effects of Hepatitis B Virus Infection on the Interferon Response in Immunodeficient Human Hepatocyte Chimeric Mice

Masataka Tsuge,[1,2,3] Shoichi Takahashi,[1,3] Nobuhiko Hiraga,[1,3] Yoshifumi Fujimoto,[1,4] Yizhou Zhang,[1,3] Fukiko Mitsui,[1,3] Hiromi Abe,[1,4] Tomokazu Kawaoka,[1,3] Michio Imamura,[1,3] Hidenori Ochi,[1,3,4] C. Nelson Hayes,[1,3] and Kazuaki Chayama[1,3,4]

[1]Department of Medicine and Molecular Science, Division of Frontier Medical Science, Programs for Biomedical Research, Graduate School of Biomedical Sciences, and [2]Live Science Division, Natural Science Center for Basic Research and Development, and [3]Liver Research Project Center, Hiroshima University; [4]Laboratory for Liver Diseases, the RIKEN Center for Genomic Medicine, Hiroshima, Japan

Complementary DNA microarray analysis of human livers cannot exclude the influence of the immunological response. In this study, complementary DNA microarray analysis was performed under immunodeficient conditions with human hepatocyte chimeric mice, and gene expression profiles were analyzed by hepatitis B virus (HBV) infection and/or interferon treatment. The expression levels of 183 of 525 genes upregulated by interferon treatment were significantly suppressed in response to HBV infection. Suppressed genes were statistically significantly associated with the interferon signaling pathway and pattern recognition receptors in the bacteria/virus recognition pathway ($P = 1.0 \times 10^{-8}$ and $P = 1.2 \times 10^{-8}$, respectively). HBV infection attenuated virus recognition and interferon response in hepatocytes, which facilitated HBV escape from innate immunity.

Chronic hepatitis B virus (HBV) infection is associated with the development of virus-related liver diseases, including chronic hepatitis, liver cirrhosis, and hepatocellular carcinoma. Interferon α (IFN-α) has been used for the treatment of chronic hepatitis B, and many large clinical trials and meta-analyses have demonstrated the effectiveness of interferon [1–3]. However, the effect of IFN-α therapy is unsatisfactory, and the molecular basis for tolerance to IFN-α is not clearly defined.

DNA microarray technology has enabled genome-wide analysis of gene transcript levels with the use of clinical tissues and animal models, which has yielded insights into the molecular features of several liver diseases [4–6]. However, it has been difficult to determine whether the changes in gene expression were caused by viral interference or by the human immune response, because all of these studies that used clinical and experimental samples were analyzed under the influence of adaptive immune responses. Recently, Mercer and colleagues developed a human hepatocyte chimeric mouse model [7]. These mice were derived from severe combined immunodeficiency (SCID) mice, which are severely immunocompromised, and the mouse liver cells were extensively replaced with human hepatocytes [7, 8]. With the use of this chimeric mouse model, in which HBV can continuously infect human hepatocytes, the effect of drugs and the response of viral infection can be analyzed in human hepatocytes under immunodeficient conditions [9]. In this study, we performed microarray analysis with human hepatocyte chimeric mouse livers to assess the direct impacts of HBV infection and IFN treatments on gene expression profiles. We successfully demonstrated that HBV infection attenuated the expression of IFN-stimulating genes under immunodeficient conditions, which suggests that HBV proteins might afford escape mechanisms from cellular innate immunity.

METHODS

A serum sample was obtained from a HBV carrier after obtaining written informed consent for the donation and evaluation of the blood sample. The inoculum was positive for Hepatitis B surface and Hepatitis B e antigens, with slightly elevated levels of serum alanine aminotransferase and high-level viremia (HBV DNA load, 7.1 log copies/mL). The studied patient was infected with HBV genotype C. The experimental protocol conformed to the ethical guidelines of the Declaration of Helsinki and was approved by the Hiroshima University Hospital ethical committee (approval ID: D08-9).

The $uPA^{+/+}/SCID^{+/+}$ mice were prepared and the human hepatocytes were transplanted as described elsewhere [8]. The experiments were performed in accordance with the guidelines of the local committee for animal experiments at Hiroshima University.

Sixteen chimeric mice, in which >90% of the liver tissue was replaced with human hepatocytes, were divided into

Received 8 December 2010; accepted 2 March 2011.
Potential conflicts of interest: none reported.
Correspondence: Kazuaki Chayama, MD, PhD, Department of Medical and Molecular Science, Division of Frontier Medical Science, Programs for Biomedical Research, Graduate School of Biomedical Science, Hiroshima University, 1-2-3 Kasumi, Minami-ku, Hiroshima 734-8551, Japan (chayama@hiroshima-u.ac.jp).

The Journal of Infectious Diseases 2011;204:224–8

0022-1899 (print)/1537-6613 (online)/2011/2042-0010$14.00
DOI: 10.1093/infdis/jir247

4 experimental groups. Group A contained 4 mice that were neither infected with HBV nor treated with IFN. Group B consisted of 3 mice that were treated with IFN-α for 6 h (7,000 IU per gram of body weight) just before being humanely killed but were not infected with HBV. Mice in groups C and D were inoculated via the mouse tail vein with human serum containing 6×10^6 copies of HBV. After inoculation, we collected mouse serum samples every 2 weeks and analyzed HBV DNA titers by real-time polymerase chain reaction (PCR) and human albumin levels by means of a human albumin enzyme-linked immunosorbent assay quantitation kit (Bethyl Laboratories), as described elsewhere [9]. Virus and human albumin titer levels are shown in Supplementary data 1. All 9 mice developed measurable viremia 4 weeks after inoculation. Eight weeks after inoculation, 4 of the 9 infected mice (group C) were humanely killed without IFN treatment and the remaining 5 mice (group D) were humanely killed after 6 h of IFN-α treatment (7,000 IU per gram of body weight). The mice were infected, had serum samples extracted, and were killed humanely under ether anesthesia, as described elsewhere [8].

All 16 chimeric mice were killed humanely, and human hepatocytes were finely dissected from the mouse livers and stored in liquid nitrogen after submerging in RNA later solution (Applied Biosystems). Total RNA was extracted with TRIzol reagent (Invitrogen) and labeled with cyanine 3 by use of a low RNA input linear amplification kit (Agilent Technologies) after amplification. Cyanine-3–labeled complimentary RNA was hybridized to a 44-K whole human genome oligo microarray (Agilent). Detailed protocols are described in Supplementary data 2.

Gene expression profiles were analyzed using GeneSpring GX software (version 10.0.2; Tomy Digital Biology). The detailed protocol is described in Supplementary data table 3. Complete linkage hierarchical clustering analysis was applied using Euclidean distance, and differentially expressed genes were annotated using information from the Gene Ontology (GO) Consortium. Global molecular networks and comparisons of canonical pathways were generated using Ingenuity Pathway Analysis (IPA) software (version 8.6; Ingenuity Systems).

Total RNA was extracted from the implanted human hepatocytes in the mouse livers by use of an RNeasy mini kit (Qiagen) and was reverse transcribed. The selected messenger RNA (mRNA) was quantified by real-time PCR using the 7300 real-time PCR system (Applied Biosystems), and the expression of glyceraldehyde-3-phosphate dehydrogenase served as a control. The amplification protocol and primer sequences are described in Supplementary data 4 and 5.

RESULTS

To analyze the direct effects of IFN in human hepatocytes, we compared the gene expression profiles between groups A (mice without IFN treatment) and B (mice with IFN treatment). Of the 1403 genes that remained after screening with the Welch *T* test, 685 genes showed a >3.0-fold change between groups. Of these 685 genes, 525 genes were up-regulated and the other 160 genes down-regulated by IFN. The top 20 IFN-regulated genes are listed in Supplementary data table 6. GO analysis revealed that 8 (40%) of the top 20 genes that were upregulated with IFN treatment were related to immune response.

To analyze the effect of HBV infection in human hepatocytes, we compared the gene expression profiles between groups A (mice without HBV infection) and C (mice with HBV infection). Among the 1,714 genes hat remained after screening, 373 genes showed a >3.0-fold change between groups. Of these 373 genes, 159 genes were up-regulated and the other 214 genes down-regulated by HBV. The top 20 HBV-regulated genes are listed in Supplementary data table 7. Several oncogenic genes such as growth differentiation factor 15 and glial cell derived neurotrophic factor were included in the top group. Most of the top 20 genes that were downregulated with HBV infection were associated with transcriptional regulation.

To examine whether HBV infection may alter the effect of IFN response in human hepatocytes, we compared gene expression profiles among all groups. As mentioned above, 525 genes were upregulated by >3.0-fold by IFN in the absence of HBV infection. A comparison of groups C (mice with HBV infection but no IFN treatment) and D (mice with both HBV infection and IFN treatment) revealed that 183 (34.9%) of the 525 genes showed statistically significantly reduced IFN response with HBV infection ($P < .01$) (Supplementary data 8A). The top 20 genes in which IFN response was significantly changed by HBV infection are shown in Table 1. The mRNA expression levels of 11 selected genes among the 183 genes with reduced IFN response were also analyzed by real-time PCR, and the reductions in IFN response by HBV infection were verified (Supplementary data 8B). Additionally, we used IPA software to analyze the influence of HBV infection on the IFN response of these 183 genes by means of a pathway-oriented approach. Pathway analysis revealed that several pathways were affected by HBV infection (Table 2). The IFN response was statistically significantly attenuated by HBV infection in the pathways related to IFN signaling and pattern recognition of bacteria and viruses ($P = 1.0 \times 10^{-8}$ and $P = 1.2 \times 10^{-8}$, respectively).

DISCUSSION

Elsewhere we have demonstrated a human hepatocyte chimeric mouse model that can be chronically infected with hepatitis B and C viruses [9–11]. This mouse model facilitates analysis of the effect of viral infection and the response to medication under immunodeficient conditions. In this study, we performed complementary DNA microarray analysis using the chimeric mouse model and obtained gene expression profiles to analyze

Table 1. Genes With Interferon Responsiveness Downregulated by Hepatitis B Virus (HBV) Infection

Gene symbol	GenBank accession no.	Function	Fold change in expression level		*P*
			Without HBV infection	With HBV infection	
ENST00000322831	None	Unknown	4.52	−1.45	4.15×10^{-7}
AA593970	AA593970	EST	9.70	1.61	5.58×10^{-7}
THC2533996	None	Unknown	3.74	−2.50	6.97×10^{-7}
LOC388532	None	Unknown	3.11	−2.48	1.61×10^{-6}
ZNF267	NM_003414	Transcription regulator	7.66	1.79	2.30×10^{-6}
ZNF217	NM_006526	Transcription regulator	3.69	1.03	3.62×10^{-6}
CRSP3	NM_015979	Transcription regulator	7.50	−1.02	4.06×10^{-6}
MGC39372	BC025340	Hypothetical protein	30.92	7.03	5.74×10^{-6}
BF972140	BF972140	EST	16.91	4.71	5.78×10^{-6}
LOC731599	XR_015536	Hypothetical protein	3.17	−4.18	8.58×10^{-6}
LOC645676	AK126559	Hypothetical protein	3.76	1.35	9.13×10^{-6}
THC2650457	None	Unknown	78.07	6.28	1.29×10^{-5}
ZNF24	NM_006965	Transcription regulator	3.69	1.36	1.64×10^{-5}
CCDC68	NM_025214	Unknown	5.88	−2.83	1.89×10^{-5}
SP110	NM_004510	Transcription regulator	5.00	10.77	2.00×10^{-5}
FLJ21272	AK024925	Hypothetical protein	14.70	2.49	3.18×10^{-5}
PLEKHF1	NM_024310	Unknown	6.65	1.84	4.70×10^{-5}
AK026418	AK026418	Unknown	9.50	2.58	5.02×10^{-5}
hCG_1790262	XM_001133847	Unknown	3.13	−2.94	6.25×10^{-5}
CEBPD	NM_005195	Transcription regulator	8.16	1.56	7.03×10^{-5}
FLJ20273	NM_019027	RNA binding	3.37	1.11	7.11×10^{-5}

NOTE. *P* values were analyzed by the Welch *T* test. *CEBPD,* CCAAT/enhancer binding protein (C/EBP) delta; *CCDC68,* coiled-coil domain containing 68; *CRSP3,* mediator complex subunit 23 (*MED23*); EST, expressed sequence tag; *FLJ20273,* RNA binding motif protein 47 (*RBM47*); *PLEKHF1,* pleckstrin homology domain containing, family F (with FYVE domain) member 1; *SP110,* SP110 nuclear body protein; *ZNF24,* zinc finger protein 24; *ZNF217,* zinc finger protein 217; *ZNF267,* zinc finger protein 267.

the direct influence of HBV infection and IFN-α treatment on human hepatocytes.

To avoid contamination with mouse tissue, human hepatocyte chimeric mice, in which liver tissue is largely (>90%) replaced by human hepatocytes, were used in the present study. However, a small amount of mouse-derived cells, such as interstitial cells, bile duct cells, and vascular cells, still remain in the chimeric mouse livers. Because of high homology between the human and mouse genomes, the signals from microarray analyses may be influenced by cross-hybridization with mouse mRNA. It is difficult to produce $uPA^{+/+}/SCID^{+/+}$ mice >10 weeks old without hepatocyte transplantation, and a previous study demonstrated that it is feasible to use microarray analysis in a functional genomics analysis of chimeric mice [12]. Therefore, to compensate for the contamination, the mice in group A, which were neither infected with HBV nor treated with IFN, were used as negative controls.

To analyze the effect of IFN treatment, we compared gene expression profiles between groups A (mice without IFN treatment) and B (mice with IFN treatment); 525 genes with >3.0-fold upregulation following IFN treatment were observed. Among them, chemokine (C-X-C motif) ligand 9, chemokine (C-X-C motif) ligand 10, and chemokine (C-X-C motif) ligand 11, which promote T cell adhesion, were remarkably highly induced with IFN treatment (Supplementary data table 6) [13]. These results suggest that the antiviral effects of IFN might involve not only direct activation of IFN-stimulated proteins such as myxovirus resistance protein A and double strand RNA-dependent protein kinase but also activation of immunity via chemokines.

Second, we compared the profiles between groups A (mice without HBV infection) and C (mice with HBV infection). As shown in Supplementary data table 7, more than half (12) of the top 20 genes upregulated by HBV infection localized to the cell membrane or the extracellular region, but 14 (70%) of the 20 downregulated genes localized to the nucleus. In addition, GO analysis demonstrated that genes related to cell cycle and DNA modification were affected by HBV infection. We speculate that HBV infection promotes cell growth and DNA damage in the hepatocyte nucleus and activates the immune response in the cytoplasm. From the clinical standpoint, some healthy HBV carriers develop hepatocellular carcinoma without chronic hepatitis or cirrhosis. The present results strongly support this observation, showing that most of the affected genes are known to be associated with carcinogenesis.

Clinically, HBV is known to develop tolerance to IFN treatment in patients with chronic hepatitis B, although the mechanism is not clear. We analyzed the IFN response with and

Table 2. Pathway Analysis of 183 Interferon-Induced Genes With Interferon Responsiveness Downregulated by Hepatitis B Virus Infection

Canonical pathways	*P*	Genes
Interferon signaling	1.00×10^{-8}	*IFIT3, SOCS1, IFIT1, MX1, IFNGR1, JAK2, STAT1, TAP1, IRF1*
Role of pattern recognition receptors in recognition of bacteria and viruses	1.20×10^{-8}	*IL12A, OAS2, OAS3*(includes EG:4940), *IFIH1, PIK3R3, TLR4, NOD2, TICAM1, DDX58, CASP1, NOD1, TLR3, RIPK2*
Type 1 diabetes mellitus signaling	2.00×10^{-4}	*SOCS1, IL12A, RIPK1, GAD1, SOCS6, SOCS2, IFNGR1, JAK2, STAT1, IRF1*
Prolactin signaling	2.70×10^{-4}	*PIK3R3, SOCS1, SOCS6, SOCS2, NMI, JAK2, STAT1, IRF1*
TREM1 signaling	3.50×10^{-4}	*TLR4, NOD2, ICAM1, CASP1, JAK2, TLR3, CASP5*
Production of nitric oxide and reactive oxygen species in macrophages	3.90×10^{-4}	*PIK3R3, TLR4, RND3, PPP2R2A, PPM1J, RHOU, IFNGR1, MAP3K8, IRF8, JAK2, STAT1, IRF1*
Pathogenesis of multiple sclerosis	1.10×10^{-3}	*CXCL10, CXCL9, CXCL11*
Activation of IRF by cytosolic pattern recognition receptors	2.60×10^{-3}	*IFIH1, RIPK1, DDX58, STAT1, IFIT2, ISG15*
Dendritic cell maturation	2.60×10^{-3}	*B2M, PIK3R3, TLR4, ICAM1, IL12A, IL1RN, IRF8, JAK2, TLR3, STAT1*
Interleukin 12 signaling and production in macrophages	3.60×10^{-3}	*PIK3R3, TLR4, IL12A, IFNGR1, MAP3K8, IRF8, STAT1, IRF1*
Sphingosine-1-phosphate signaling	3.60×10^{-3}	*PIK3R3, S1PR2, RND3, CASP1, RHOU, CASP4, CASP7, CASP5*
JAK-STAT signaling	4.00×10^{-3}	*PIK3R3, SOCS1, SOCS6, SOCS2, JAK2, STAT1*
Growth hormone signaling	4.70×10^{-3}	*PIK3R3, SOCS1, SOCS6, SOCS2, JAK2, STAT1*
Retinoic acid mediated apoptosis signaling	8.50×10^{-3}	*TNFRSF10B, PARP8, TNFSF10, TIPARP, IRF1*

NOTE. *B2M,* beta-2-microglobulin; *CASP1,* caspase 1, apoptosis-related cysteine peptidase (interleukin 1, beta, convertase); *CASP4,* caspase 4, apoptosis-related cysteine peptidase; *CASP5,* caspase 5, apoptosis-related cysteine peptidase; *CASP7,* caspase 7, apoptosis-related cysteine peptidase; *CXCL9,* chemokine (C-X-C motif) ligand 9; *CXCL10,* chemokine (C-X-C motif) ligand 10; *CXCL11,* chemokine (C-X-C motif) ligand 11; *DDX58,* DEAD (Asp-Glu-Ala-Asp) box polypeptide 58; *GAD1,* glutamate decarboxylase 1 (brain, 67kDa); *ICAM1,* intercellular adhesion molecule 1; *IFIH1,* interferon induced with helicase C domain 1; *IFIT1,* interferon-induced protein with tetratricopeptide repeats 1; *IFIT2,* interferon-induced protein with tetratricopeptide repeats 2; *IFIT3,* interferon-induced protein with tetratricopeptide repeats 3; *IFNGR1,* interferon gamma receptor 1; *IL1RN,* interleukin 1 receptor antagonist; *IL12A,* interleukin 12A (natural killer cell stimulatory factor 1, cytotoxic lymphocyte maturation factor 1, p35); IRF, interferon regulatory factor; *IRF1,* interferon regulatory factor 1; *IRF8,* interferon regulatory factor 8; *ISG15,* ISG15 ubiquitin-like modifier; *JAK2,* Janus kinase 2; *MAP3K8,* mitogen-activated protein kinase kinase kinase 8; *MX1,* myxovirus (influenza virus) resistance 1, interferon-inducible protein p78 (mouse); *NMI,* N-myc (and STAT) interactor; *NOD1,* nucleotide-binding oligomerization domain containing 1; *NOD2,* nucleotide-binding oligomerization domain containing 2; *OAS2,* 2′-5′-oligoadenylate synthetase 2, 69/71kDa; *OAS3,* 2′-5′-oligoadenylate synthetase 3, 100kDa; *PARP8,* poly (ADP-ribose) polymerase family, member 8; *PIK3R3,* phosphoinositide-3-kinase, regulatory subunit 3 (gamma); *PPM1J,* protein phosphatase, Mg2+/Mn2+ dependent, 1J; *PPP2R2A,* protein phosphatase 2, regulatory subunit B, alpha; *RHOU,* ras homolog gene family, member U; *RIPK1,* receptor (TNFRSF)-interacting serine-threonine kinase 1; *RIPK2,* receptor-interacting serine-threonine kinase 2; *RND3,* Rho family GTPase 3; *S1PR2,* sphingosine-1-phosphate receptor 2; *SOCS1,* suppressor of cytokine signaling 1; *SOCS2,* suppressor of cytokine signaling 2; *SOCS6,* suppressor of cytokine signaling 6; *STAT1,* signal transducer and activator of transcription 1, 91kDa; *TAP1,* transporter 1, ATP-binding cassette, sub-family B (MDR/TAP); *TICAM1,* Toll-like receptor adaptor molecule 1; *TIPARP,* TCDD-inducible poly(ADP-ribose) polymerase; *TLR3,* Toll-like receptor 3; *TLR4,* Toll-like receptor 4; *TNFRSF10B,* tumor necrosis factor receptor superfamily, member 10b; *TNFSF10,* tumor necrosis factor (ligand) superfamily, member 10; *TREM1,* triggering receptor expressed on myeloid cells 1.

without HBV infection, focusing on the 525 upregulated genes with IFN treatment and using all obtained gene expression profiles. Interestingly, 61.3% of the extracted genes maintained an IFN response, but in 34.9% of those genes, IFN responses were attenuated by HBV infection (Supplementary data 8A). Genes corresponding to interferon signaling, including suppressor of cytokine signaling 1 (*SOCS1*) and interferon regulatory factor 1, and those corresponding to pattern recognition of bacteria and viruses, including nucleotide-binding oligomerization domain containing 1 (*NOD1*) and receptor-interacting serine-threonine kinase 2 (*RIPK2*), were statistically significantly associated with HBV-mediated attenuation to IFN response ($P = 1.0 \times 10^{-8}$ and $P = 1.2 \times 10^{-8}$, respectively). According to these results, HBV infection significantly up-regulated *SOCS1* expression and reduced the IFN responsiveness of *SOCS1*. Thus, *SOCS1* might support chronic infection of HBV in escaping the effects of innate immunity or IFN therapy. On the other hand, genes involved in recognition of viral infection were also inhibited following HBV infection. Both *NOD1* and *RIPK2* are related to innate and adaptive immune responses [14, 15]. We speculated that inhibition of *NOD1* or *RIPK2* expression facilitates HBV survival. Although further study is needed, these results may have important implications for the mechanisms of viral escape from innate immunity.

In conclusion, we performed complementary DNA microarray analysis using human hepatocyte chimeric mice. With this system, we could analyze the direct effects of IFN treatment and HBV infection without the confounding effects of the lymphocyte immunological response and obtained evidence that HBV infection attenuated the virus recognition and IFN response in

hepatocytes, by which means HBV could evade innate immune detection and response.

Supplementary Data

Supplementary data are available at *The Journal of Infectious Diseases* online.

Funding

This work was supported by the Ministry of Education, Sports, Culture and Technology and the Ministry of Health, Labor and Welfare (Grants-in-Aid for scientific research and development).

Acknowledgments

This work was performed at the Research Center for Molecular Medicine, Faculty of Medicine, Hiroshima University. We thank Mari Shiota, Rie Akiyama, and Ruri Mikami for their excellent technical assistance and Aya Furukawa for clerical assistance. The funders had no role in the study design, data collection and analysis, decision to publish, or preparation of the manuscript.

References

1. Hsu HY, Tsai HY, Wu TC, et al. Interferon-alpha treatment in children and young adults with chronic hepatitis B: a long-term follow-up study in Taiwan. Liver Int **2008**; 28:1288–97.
2. Lin SM, Tai DI, Chien RN, Sheen IS, Chu CM, Liaw YF. Comparison of long-term effects of lymphoblastoid interferon alpha and recombinant interferon alpha-2a therapy in patients with chronic hepatitis B. J Viral Hepat **2004**; 11:349–57.
3. Sung JJ, Tsoi KK, Wong VW, Li KC, Chan HL. Meta-analysis: treatment of hepatitis B infection reduces risk of hepatocellular carcinoma. Aliment Pharmacol Ther **2008**; 28:1067–77.
4. Bigger CB, Brasky KM, Lanford RE. DNA microarray analysis of chimpanzee liver during acute resolving hepatitis C virus infection. J Virol **2001**; 75:7059–66.
5. Honda M, Yamashita T, Ueda T, Takatori H, Nishino R, Kaneko S. Different signaling pathways in the livers of patients with chronic hepatitis B or chronic hepatitis C. Hepatology **2006**; 44:1122–38.
6. Okabe H, Satoh S, Kato T, et al. Genome-wide analysis of gene expression in human hepatocellular carcinomas using cDNA microarray: identification of genes involved in viral carcinogenesis and tumor progression. Cancer Res **2001**; 61:2129–37.
7. Mercer DF, Schiller DE, Elliott JF, et al. Hepatitis C virus replication in mice with chimeric human livers. Nat Med **2001**; 7:927–33.
8. Tateno C, Yoshizane Y, Saito N, et al. Near completely humanized liver in mice shows human-type metabolic responses to drugs. Am J Pathol **2004**; 165:901–12.
9. Tsuge M, Hiraga N, Takaishi H, et al. Infection of human hepatocyte chimeric mouse with genetically engineered hepatitis B virus. Hepatology **2005**; 42:1046–54.
10. Hiraga N, Imamura M, Tsuge M, et al. Infection of human hepatocyte chimeric mouse with genetically engineered hepatitis C virus and its susceptibility to interferon. FEBS Lett **2007**; 581:1983–7.
11. Kimura T, Imamura M, Hiraga N, et al. Establishment of an infectious genotype 1b hepatitis C virus clone in human hepatocyte chimeric mice. J Gen Virol **2008**; 89:2108–13.
12. Walters KA, Joyce MA, Thompson JC, et al. Application of functional genomics to the chimeric mouse model of HCV infection: optimization of microarray protocols and genomics analysis. Virol J **2006**; 3:37.
13. Luster AD, Jhanwar SC, Chaganti RS, Kersey JH, Ravetch JV. Interferon-inducible gene maps to a chromosomal band associated with a (4;11) translocation in acute leukemia cells. Proc Natl Acad Sci U S A **1987**; 84:2868–71.
14. Tong HH, Long JP, Li D, DeMaria TF. Alteration of gene expression in human middle ear epithelial cells induced by influenza A virus and its implication for the pathogenesis of otitis media. Microb Pathog **2004**; 37:193–204.
15. Viala J, Chaput C, Boneca IG, et al. Nod1 responds to peptidoglycan delivered by the *Helicobacter pylori* cag pathogenicity island. Nat Immunol **2004**; 5:1166–74.

In Vivo Adaptation of Hepatitis C Virus in Chimpanzees for Efficient Virus Production and Evasion of Apoptosis

Mohsan Saeed,[1,2] Masaaki Shiina,[3] Tomoko Date,[1] Daisuke Akazawa,[1] Noriyuki Watanabe,[1] Asako Murayama,[1] Tetsuro Suzuki,[1] Haruo Watanabe,[2,4] Nobuhiko Hiraga,[5] Michio Imamura,[5] Kazuaki Chayama,[5] Youkyung Choi,[6] Krzysztof Krawczynski,[6] T. Jake Liang,[7] Takaji Wakita,[1] and Takanobu Kato[1]

Hepatitis C virus (HCV) employs various strategies to establish persistent infection that can cause chronic liver disease. Our previous study showed that both the original patient serum from which the HCV JFH-1 strain was isolated and the cell culture–generated JFH-1 virus (JFH-1cc) established infection in chimpanzees, and that infected JFH-1 strains accumulated mutations after passage through chimpanzees. The aim of this study was to compare the *in vitro* characteristics of JFH-1 strains emerged in each chimpanzee at early and late stages of infection, as it could provide an insight into the phenomenon of viral persistence. We generated full-genome JFH-1 constructs with the mutations detected in patient serum-infected (JFH-1/S1 and S2) and JFH-1cc–infected (JFH-1/C) chimpanzees, and assessed their effect on replication, infectious virus production, and regulation of apoptosis in cell culture. The extracellular HCV core antigen secreted from JFH-1/S1-, S2-, and C-transfected HuH-7 cells was 2.5, 8.9, and 2.1 times higher than that from JFH-1 wild-type (JFH-1/wt) transfected cells, respectively. Single cycle virus production assay with a CD81-negative cell line revealed that the strain JFH-1/S2, isolated from the patient serum-infected chimpanzee at a later time point of infection, showed lower replication and higher capacity to assemble infectious virus particles. This strain also showed productive infection in human hepatocyte–transplanted mice. Furthermore, the cells harboring this strain displayed lower susceptibility to the apoptosis induced by tumor necrosis factor α or Fas ligand compared with the cells replicating JFH-1/wt. *Conclusion:* The ability of lower replication, higher virus production, and less susceptibility to cytokine-induced apoptosis may be important for prolonged infection *in vivo*. Such control of viral functions by specific mutations may be a key strategy for establishing persistent infection. (HEPATOLOGY 2011;54:425-433)

Currently, approximately 200 million people are infected with hepatitis C virus (HCV) and are at continuous risk of developing chronic liver diseases such as chronic hepatitis, liver cirrhosis, and hepatocellular carcinoma.[1,2] Although acute HCV infection elicits innate and adaptive immune responses, the virus successfully evades clearance in approximately 75% of infected individuals.[3,4] The mechanisms by

Abbreviations: Ag, antigen; CTL, cytotoxic T lymphocytes; FasL, Fas ligand; HCV, hepatitis C virus; JFH-1cc, cell culture–generated JFH-1 virus; JFH-1/wt, JFH-1 wild-type; MFI, mean fluorescence intensity; NK, natural killer; NS, nonstructural; PARP, poly(adenosine diphosphate ribose) polymerase; TNF-α, tumor necrosis factor α; TUNEL, terminal deoxynucleotidyl transferase–mediated deoxyuridine triphosphate nick-end labeling.

From the [1]Department of Virology II, National Institute of Infectious Diseases, Tokyo, Japan; the [2]Department of Infection and Pathology, Graduate School of Medicine, The University of Tokyo, Tokyo, Japan; the [3]Division of Gastroenterology, Tohoku University Graduate School of Medicine, Sendai, Japan; the [4]National Institute of Infectious Diseases, Tokyo, Japan; the [5]Department of Medicine and Molecular Science, Division of Frontier Medical Science, Programs for Biomedical Research, Graduate School of Biomedical Sciences, Hiroshima University, Hiroshima, Japan; the [6]Division of Viral Hepatitis, Center for Disease Control and Prevention, Atlanta, GA; and the [7]Liver Diseases Branch, National Institute of Diabetes and Digestive and Kidney Diseases, National Institutes of Health, Bethesda, MD.

Received November 26, 2010; accepted April 18, 2011.

Supported by grants-in-aid from the Japan Society for the Promotion of Science, the Ministry of Health, Labor, and Welfare of Japan, and the Ministry of Education, Culture, Sports, Science, and Technology, by the Research on Health Sciences Focusing on Drug Innovation from the Japan Health Sciences Foundation, and in part by the Intramural Research Program of the NIDDK, NIH (T. J. L.).

Tetsuro Suzuki is currently affiliated with the Department of Infectious Diseases, Hamamatsu University School of Medicine, Hamamatsu, Japan.

Address reprint requests to: Takanobu Kato, M.D., Ph.D., Department of Virology II, National Institute of Infectious Diseases, Tokyo, 162-8640, Japan. E-mail: takato@nih.go.jp; fax: (81)-3-5285-1161.

View this article online at wileyonlinelibrary.com.

DOI 10.1002/hep.24399

Potential conflict of interest: Nothing to report.

Additional Supporting Information may be found in the online version of this article.

which HCV leads to persistent infection at a high frequency are not yet fully understood. Lack of appropriate animal models, except chimpanzees, has rendered such studies difficult. Human hepatocyte-transplanted mice,[5,6] a useful small animal model to study HCV infection, are unsuitable to study the mechanisms of virus persistence because of a lack of B and T cell–mediated immunity.

HCV is a noncytopathic positive-stranded RNA virus of the *Flaviviridae* family. It primarily infects hepatocytes of humans and chimpanzees, where, thanks to error-prone RNA-dependent RNA polymerase, the infected virus accumulates a high number of mutations rapidly, thus providing opportunity for selection of viruses that have the ability to escape the immune system and establish persistent infection. Deciphering the strategies employed by HCV to establish persistence can be helpful in the development of new strategies to eradicate the virus and to stop disease progression. Until recently, the lack of an HCV strain having the ability to establish infection *in vivo* and *in vitro* was a substantial hindrance in studying the molecular mechanisms of virus persistence. This problem was solved by the identification of an HCV strain, JFH-1, that was isolated from a fulminant hepatitis patient and found to be capable of replicating and assembling infectious virus particles in chimpanzees as well as in cell culture.[7-10] This clone can be used to study the molecular mechanisms by which HCV evades the host immune system and causes chronic infection.

In a previous report, we inoculated patient serum from which the JFH-1 strain was originally isolated and cell culture–generated JFH-1 virus (JFH-1cc) into two different chimpanzees.[11] HCV established infection in both animals within 3 days of inoculation. In the JFH-1cc–infected chimpanzee, genome sequence of predominant infecting virus at week 2 was identical to JFH-1 wild-type (JFH-1/wt [in this study, this abbreviation was used instead of JFH-1 to distinguish it from other variant strains]), and the infecting virus has four synonymous and seven nonsynonymous mutations at week 7. In the JFH-1 patient serum–infected chimpanzee, 19 synonymous and six nonsynonymous mutations were observed in predominantly circulating virus at week 2, and this number increased to 35 synonymous and 17 nonsynonymous mutations at the later stage of infection course (week 23).[11] From these observations, we presumed that the isolates evolved in each chimpanzee at later stages of infection might have some advantage over the viruses isolated at earlier time points for survival in infected animals. Thus, in this study, we generated JFH-1 variants containing the mutations observed in these animals and assessed their effect on replication and infectious virus production in cell culture. Furthermore, we examined the effects of infection of these strains to tumor necrosis factor α (TNF-α)– or Fas ligand (FasL)–mediated apoptosis.

Materials and Methods

The complete Materials and Methods are provided in the Supporting Information.

Results

Effects of Mutations Identified in Chimpanzees. To investigate the effect of mutations on virus phenotype, we generated constructs containing the mutations observed in JFH-1 patient serum–infected chimpanzee and JFH-1cc–infected chimpanzee at various time points. The JFH-1 variants JFH-1/S1 and JFH-1/S2 contain the mutations observed in the patient serum–infected chimpanzee at week 2 and week 23, respectively, and JFH-1/C contains the mutations observed in the JFH-1cc–infected chimpanzee at week 7 (Supporting Table 1). The replication and virus production capacity of these variants in HuH-7 cells was compared with that of JFH-1/wt. After electroporation of *in vitro*–synthesized full-genome RNA of JFH-1/wt and variant strains, extracellular and intracellular HCV RNA and core antigen (Ag) were measured (Fig. 1). At day 5 posttransfection, all constructs displayed similar intracellular HCV RNA levels. However, extracellular HCV RNA level of JFH-1/C was 1.6 times higher than that of JFH-1/wt. Likewise, extracellular HCV RNA level of JFH-1/S2 was 3.4 times higher than that of JFH-1/S1 (Fig. 1A). Intracellular HCV core Ag levels of JFH-1/S2 and C were 240.9 ± 58.2 and 189.8 ± 42.1 fmol/mg protein, respectively, and were significantly lower ($P < 0.005$) than that of JFH-1/S1 (526.1 ± 58.2 fmol/mg protein) and JFH-1/wt (511.7 ± 32.9 fmol/mg protein) at day 1, but reached comparable levels at day 5 posttransfection. On the other hand, extracellular HCV core Ag level of JFH-1/C was 2.2 times higher than that of JFH-1/wt, and that of JFH-1/S2 was 3.6 times higher than that of JFH-1/S1 at day 5 posttransfection (Fig. 1B). Transfection efficiency of these strains, indicated by intracellular HCV core Ag levels at 4 hours posttransfection, was almost identical (data not shown).

Single Cycle Virus Production Assay. For detailed analysis of the effects of these mutations on different stages of the virus lifecycle, we used a Huh7-25 cell

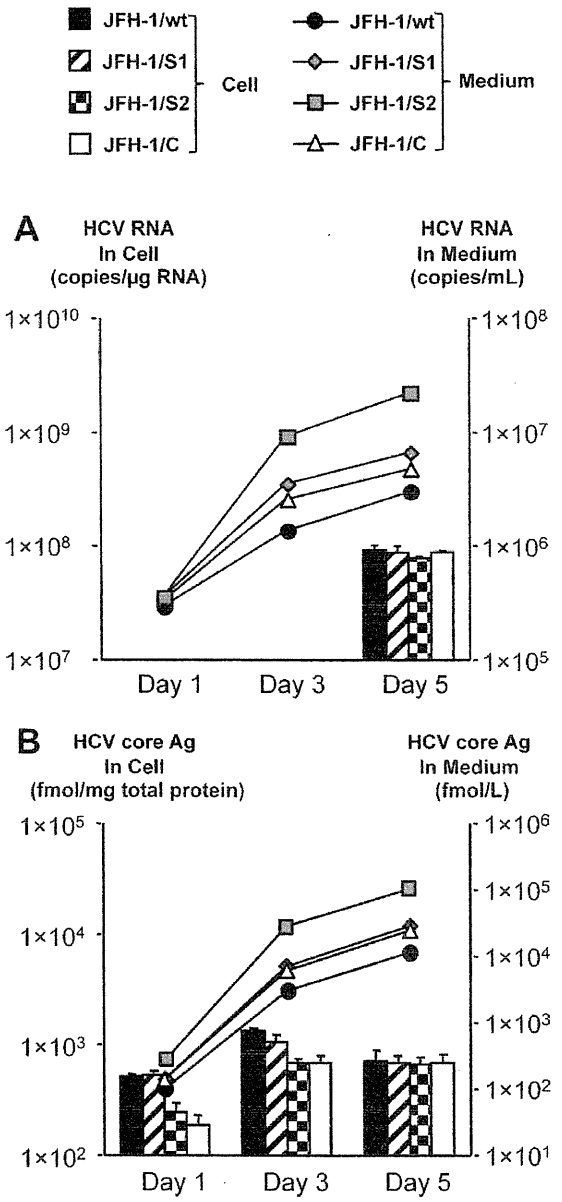

Fig. 1. Effects of *in vivo* adaptive mutations on virus production in HuH-7 cells. One million cells were transfected with 10 μg *in vitro*-transcribed RNA of JFH-1/wt, JFH-1/S1, JFH-1/S2, and JFH-1/C. (A) HCV RNA and (B) core Ag levels in cell lysates and medium were measured at the indicated time points. Assays were performed in triplicate, and data are presented as the mean ± SD.

line that lacks the surface expression of CD81, one of the cellular receptors for HCV entry. Three days after transfection with full-genome RNA of JFH-1/wt, JFH-1/S1, JFH-1/S2, and JFH-1/C, HCV RNA levels and infectivity titer were measured, and the specific infectivity was calculated (Table 1). Intracellular HCV RNA levels of JFH-1/C and JFH-1/S2 were lower than those of JFH-1/wt and S1, suggesting lower replication efficiency of these strains. However, the intracellular infectivity titers of JFH-1/C and JFH-1/S2 were 2.03 and 11.0 times higher than those of JFH-1/wt and JFH-1/S1, respectively ($P < 0.005$). Intracellular-specific infectivities (infectivity titer/HCV RNA copy number) of JFH-1/C and JFH-1/S2 showed more pronounced difference from those of JFH-1/wt and JFH-1/S1 (3.92 times and 12.9 times higher, respectively; $P < 0.005$). The infectious virus secretion rate (extracellular infectivity titer/intracellular infectivity titer) was not significantly different between JFH-1/wt and variant strains. These data indicate that mutations identified in chimpanzees at the later time point of infection led to reduced viral replication and increased assembly of infectious virus particles without any effect on viral release in cell culture.

Subgenomic Replicon Assay. To further confirm the replication efficiencies of strains observed in chimpanzees, we generated subgenomic replicons of JFH-1/wt, JFH-1/S1, JFH-1/S2, and JFH-1/C carrying the firefly luciferase reporter gene (SGR-JFH-1/Luc/wt, SGR-JFH-1/Luc/S1, SGR-JFH-1/Luc/S2, and SGR-JFH-1/Luc/C). *In vitro*–transcribed RNAs of these constructs were transfected into HuH-7 cells, and luciferase activity was measured to assess their replication capacity. The luciferase activities of SGR-JFH-1/Luc/C and SGR-JFH-1/Luc/S2 replicons were 7.30 and 7.33 times lower than those of SGR-JFH-1/Luc/wt and SGR-JFH-1/Luc/S1, respectively, at day 1 ($P < 0.00005$), suggesting attenuated replication capacities of variant replicons isolated from each animal at later time points of infection (Supporting Fig. 1A). The luciferase activity 4 hours after transfection was comparable, indicating similar levels of transfection efficiency (data not shown). Based on these data, we found that the mutations that emerged in nonstructural (NS)3-NS5B of JFH-1/S2 and JFH-1/C reduced the replication efficiency in cell culture.

Genomic Regions Responsible for Lower Replication and Higher Assembly of JFH-1/S2. To further clarify the genomic region responsible for lower replication efficiency and higher assembly rate of JFH-1/S2, we generated the chimeric constructs JFH-1/S2-wt and JFH-1/wt-S2 as described in the Supporting Materials and Methods. *In vitro*–transcribed RNAs of JFH-1/wt, JFH-1/S2, JFH-1/S2-wt, and JFH-1/wt-S2 were introduced into HuH-7 cells by electroporation and intracellular and extracellular HCV RNA and core Ag were measured. At day 5 posttransfection, all constructs displayed comparable intracellular HCV RNA levels (Fig. 2). However, extracellular HCV RNA levels of JFH-1/S2 and JFH-1/S2-wt were significantly

Table 1. Infectious Virus Production and Release of JFH-1/wt and Variants in Huh7-25 Cells

Strain	Intracellular			Extracellular	Secretion Ratio (Extracellular/ Intracellular)
	HCV RNA (copies/μg RNA)	Infectivity Titer (ffu/well)	Specific Infectivity (ffu/copies)	Infectivity Titer (ffu/well)	
JFH-1/wt	$7.75 \times 10^8 \pm 1.04 \times 10^8$	$4.21 \times 10^2 \pm 4.32 \times 10^1$	$2.09 \times 10^{-7} \pm 7.06 \times 10^{-8}$	$1.94 \times 10^3 \pm 3.76 \times 10^1$	4.6 ± 1.3
JFH-1/S1	$7.04 \times 10^8 \pm 8.49 \times 10^7$	$4.72 \times 10^2 \pm 5.63 \times 10^1$	$2.91 \times 10^{-7} \pm 6.00 \times 10^{-8}$	$3.02 \times 10^3 \pm 2.77 \times 10^2$	5.4 ± 2.0
JFH-1/S2	$4.16 \times 10^{8**} \pm 7.47 \times 10^6$	$5.19 \times 10^{3**} \pm 8.24 \times 10^1$	$3.76 \times 10^{-6**} \pm 7.01 \times 10^{-7}$	$3.23 \times 10^{4**} \pm 3.52 \times 10^3$	6.2 ± 3.0
JFH-1/C	$3.15 \times 10^{8*} \pm 5.02 \times 10^7$	$8.59 \times 10^{2*} \pm 4.81 \times 10^1$	$8.19 \times 10^{-7*} \pm 5.68 \times 10^{-8}$	$3.68 \times 10^3 \pm 3.02 \times 10^3$	4.3 ± 1.4
JFH-1/S2-wt	$7.07 \times 10^8 \pm 8.43 \times 10^7$	$4.40 \times 10^{3*} \pm 9.5 \times 10^1$	$2.73 \times 10^{-6*} \pm 2.35 \times 10^{-7}$	$3.0 \times 10^{4*} \pm 1.1 \times 10^3$	6.7 ± 0.7
JFH-1/wt-S2	$4.21 \times 10^{8*} \pm 1.97 \times 10^7$	$2.7 \times 10^2 \pm 2.9 \times 10^1$	$2.02 \times 10^{-7} \pm 4.0 \times 10^{-8}$	$1.7 \times 10^3 \pm 1.3 \times 10^2$	4.5 ± 0.4

Abbreviation: ffu, focus-forming units.
*$P < 0.005$ versus JFH-1/wt.
**$P < 0.005$ versus JFH-1/S1.

higher ($P < 0.0005$) than that of JFH-1/wt. On the other hand, extracellular RNA level of JFH-1/wt-S2 chimeric construct was lower than that of JFH-1/S2 and JFH-1/S2-wt and similar to that of JFH-1/wt. Likewise, extracellular core Ag levels of JFH-1/S2 and JFH-1/S2-wt were also significantly higher than that of JFH-1/wt. Intracellular HCV core Ag levels of JFH-1/S2 and JFH-1/wt-S2 on day 1 posttransfection were 240.9 ± 58.2 and 134.3 ± 17.1 fmol/mg protein, respectively, and were significantly lower ($P < 0.005$) than that of JFH-1/wt (526.1 ± 58.2 fmol/mg protein), whereas intracellular HCV core Ag level of JFH-1/S2-wt was comparable to that of JFH-1/wt. Transfection efficiency of these strains, indicated by intracellular HCV core Ag levels at 4 hours posttransfection, was almost identical (data not shown).

To further elucidate, we transfected Huh7-25 cells with *in vitro*–transcribed RNA of JFH-1/wt, JFH-1/S2, JFH-1/S2-wt, and JFH-1/wt-S2 and measured HCV RNA, core Ag, and infectivity titer in the cells and culture medium. Intracellular HCV RNA levels of JFH-1/S2 and JFH-1/wt-S2 were similar and lower than those of JFH-1/wt and JFH-1/S2-wt, suggesting mutations in NS3-NS5B were responsible for lower replication efficiency of JFH-1/S2 (Table 1). Intracellular infectivity titer of JFH-1/S2 and JFH-1/S2-wt was 12.3 and 10.4 times higher, respectively, than that of JFH-1/wt ($P < 0.005$) on day 3 posttransfection. The intracellular specific infectivities of JFH-1/S2 and JFH-1/S2-wt were significantly higher than that of JFH-1/wt (18 times and 13.1 times higher, respectively; $P < 0.005$). On the other hand, intracellular specific infectivity of JFH-1/wt-S2 was comparable to that of JFH-1/wt. The infectious virus secretion rate was not significantly different among all the constructs (Table 1). These data indicate that mutations emerged in the core-NS2 region of JFH-1/S2 are responsible for the enhanced assembly of infectious virus particles compared with JFH-1/wt.

Mapping Study for JFH-1/S2 Strain. Because our experiments with JFH-1/S2 subgenomic replicon and JFH-1/wt-S2 chimeric construct showed that mutations emerged in the NS3-NS5B region are responsible for reduced replication efficiency of JFH-1/S2, we performed mapping studies by generating various JFH-1 subgenomic replicons, each containing the mutations observed in individual nonstructural protein. Although mutations in NS4B and NS5A were associated with attenuated replication capacity of JFH-1, the most significant decrease in replication was observed with NS5B mutations (Supporting Fig. 1B).

For detailed analysis of mutations responsible for higher assembly, *in vitro*–transcribed RNAs of JFH-1/wt, JFH-1/S2, JFH-1/S2-wt, JFH-1/N397S, JFH-1/L752V, JFH-1/S2-NS2 (containing mutations G838R, A878V, and V881A), JFH-1/G838R, and JFH-1/A878V were transfected into Huh7-25 cells, and intracellular-specific infectivities were compared (Supporting Table 2). As reported previously, JFH1/G838R showed higher intracellular specific infectivity than that of JFH-1/wt, but could not reach the level of JFH-1/S2 or JFH-1/S2-wt. Among the mutants, intracellular specific infectivities of JFH1/L752V, JFH1/NS2, and JFH1/G838R were 4.02, 5.42, and 3.07 times higher than that of JFH-1/wt, but those of JFH1/N397S and JFH1/A878V were similar to that of JFH-1/wt. Thus, the combination of mutations in P7 and NS2 was found to contribute to the higher assembly of the JFH-1/S2 strain.

Human Hepatocyte–Transplanted Mouse Assay. To assess the *in vivo* infectivity of these strains, we inoculated culture medium containing 10^7 copies (HCV RNA titer measured by RTD-PCR) of JFH-1/wt, JFH-1/S1, JFH-1/S2, and C viruses into human

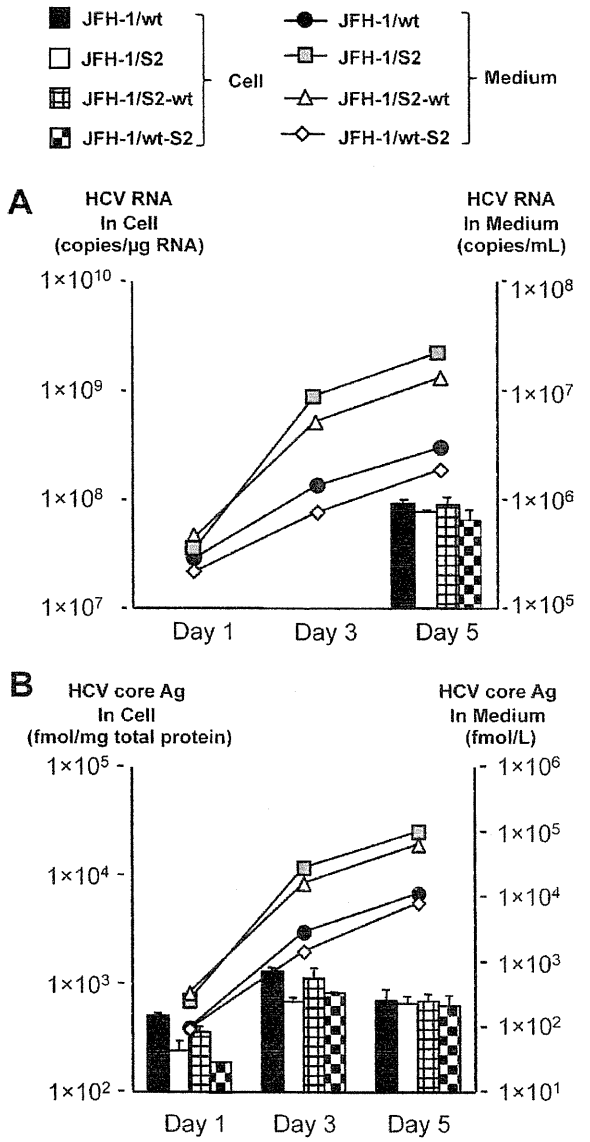

Fig. 2. Virus production of JFH-1/S2 chimeric constructs in HuH-7 cells. One million cells were transfected with 10 μg *in vitro*-transcribed RNA of JFH-1/wt, JFH-1/S2, JFH-1/S2-wt, and JFH-1/wt-S2. (A) HCV RNA and (B) core Ag levels in cell lysates and medium were measured at the indicated time points. Assays were performed in triplicate, and data are presented as the mean ± SD.

hepatocyte-transplanted mice. Two mice were used for each virus. Two weeks after intravascular inoculation, all mice but one became HCV RNA–positive (Fig. 3). Two mice died 3 weeks after inoculation; one was inoculated with JFH-1/wt and had developed infection, and the other was inoculated with JFH-1/C and died without developing infection. HCV RNA levels in infected mice fluctuated, ranging from 10^6 to 10^9 copies/mL. We could not observe much difference of infected HCV RNA titer among these inoculated mice. Sequence analyses of the complete open reading frames revealed that infecting JFH-1/wt virus and variant strains had no nonsynonymous mutations at the time of development of infection. From these data, we concluded that not only JFH-1/wt virus but also JFH-1/S1, JFH-1/S2, and JFH-1/C viruses were able to establish productive infection in human hepatocyte-transplanted mice.

Apoptosis Induction Assay. To investigate the survival strategy against the host defense system, we examined the susceptibility of JFH-1/wt and variant strains to TNF-α–mediated apoptosis induction. After transfection with *in vitro*–transcribed RNA of JFH-1/wt, JFH-1/S1, JFH-1/S2, and JFH-1/C, Huh-7.5.1 cells were exposed to TNF-α plus actinomycin D. Without exposure, apoptosis was observed in a limited number of HCV-positive cells (Supporting Fig. 2A). Forty-eight hours later, cells were harvested, fixed, and

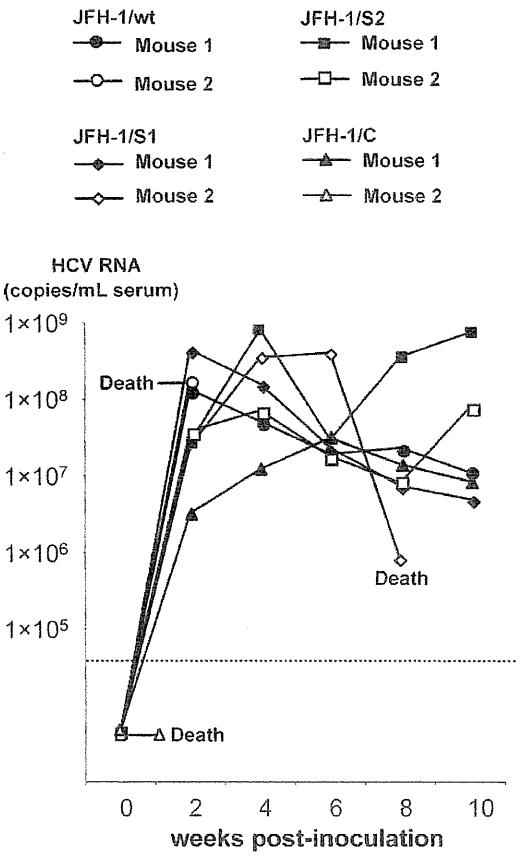

Fig. 3. *In vivo* infection study of JFH-1/wt and its variants in human hepatocyte-transplanted mice. Cell culture medium containing 1 × 10^7 HCV RNA copies of JFH-1/wt, JFH-1/S1, JFH-1/S2, and JFH-1/C were inoculated into human hepatocyte-transplanted mice, and HCV RNA levels in mice serum were monitored.

subjected to terminal deoxynucleotidyl transferase–mediated deoxyuridine triphosphate nick-end labeling (TUNEL) assay and anti-HCV NS5A staining. The effects of JFH-1/wt, JFH-1/S1, JFH-1/S2, and JFH-1/C transfection on apoptosis induction were determined by calculating the ratio of apoptosis between HCV-positive and HCV-negative populations and expressed as an apoptosis induction index. After treatment of JFH-1/wt–transfected cells with TNF-α, apoptosis was observed in 36.8% of the HCV-positive population and in 19.3% of the HCV-negative population, and the apoptosis induction index was 1.85 ± 0.06 (Fig. 4). The apoptosis induction indexes of JFH-1/S1–transfected and JFH-1/C– transfected cells were 1.23 ± 0.06 and 1.16 ± 0.10, respectively, suggesting lower susceptibility to apoptosis induction compared with JFH-1/wt. On the other hand, the apoptosis induction index of JFH-1/S2 was 0.74 ± 0.17, which was substantially lower than that of JFH-1/wt, demonstrating the more reduced apoptosis in the cells harboring this strain. Similar results were obtained by treatment with FasL plus actinomycin D (Supporting Fig. 2B). To confirm the lower susceptibility of JFH-1/S2–transfected cells, apoptosis was also detected by staining with anticleaved poly(adenosine diphosphate ribose) polymerase (PARP) antibody. The apoptosis induction indexes of JFH-1/wt and JFH-1/S2–transfected cells were 2.28 ± 0.24 and 1.15 ± 0.14, respectively, and were consistent with TUNEL assay (Fig. 5). Although the HCV NS5A-positive rate in JFH-1/S2–transfected cells was higher than that in JFH-1/wt, the mean fluorescence intensity of the NS5A-positive population in JFH-1/S2–transfected cells was significantly lower (185.0 ± 8.7) than that in JFH-1/wt–transfected cells (395.0 ± 98.0), corresponding to the observed phenotype of the JFH-1/S2 strain in the single cycle virus production assay (i.e., lower replication efficiency and rapid spread to surrounding cells).

To clarify the genomic region responsible for lower susceptibility of JFH-1/S2 to cytokine-induced apoptosis, we examined the effect of TNF-α on the cells carrying subgenomic reporter replicons. The apoptosis induction index of SGR-JFH1/Luc/S2–transfected cells was lower than that of SGR-JFH1/Luc/wt–transfected cells (Supporting Fig. 2C); however, the difference was not as pronounced as with full-genome constructs, indicating that mutations in the NS3-NS5B region contribute to lower susceptibility of JFH-1/S2 to cytokine-induced apoptosis, but they are not sufficient to explain the difference between JFH-1/wt and JFH-1/S2. We confirmed these results by use of the chimeric

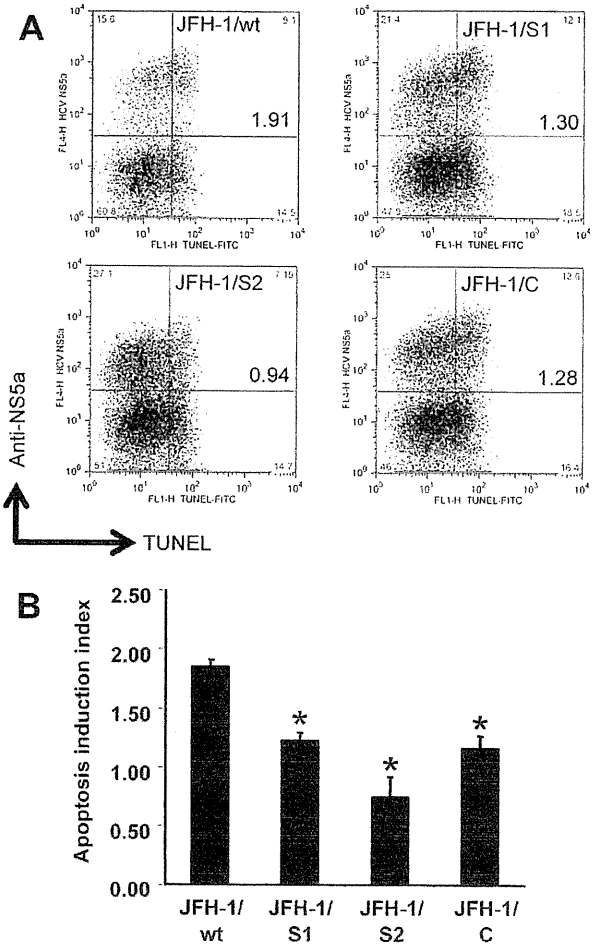

Fig. 4. Apoptosis induction in Huh-7.5.1 cells transfected with JFH-1/wt and its variants. (A) Three million cells were transfected with 3 μg *in vitro*-transcribed full-genome RNA of JFH-1/wt, JFH-1/S1, JFH-1/S2, and JFH-1/C. Forty-eight hours later, apoptosis was induced by exposing cells to 20 ng/mL TNF-α plus 50 ng/mL actinomycin D. Cells were harvested after 48 hours of treatment and subjected to TUNEL and anti-HCV NS5A staining. Dot plots show HCV replication and apoptosis at the single cell level. Quadrant gates were determined using unstained and a terminal deoxynucleotidyltrasferase-untreated control in each culture condition. The clone names and apoptosis induction indexes are indicated in the upper right box. (B) Apoptosis induction indexes of JFH-1/wt-, JFH-1/S1-, JFH-1/S2-, and JFH-1/C- transfected cells. The mean ± SD of three independent experiments is shown. $^*P < 0.005$ versus JFH-1/wt.

constructs JFH-1/S2-wt and JFH-1/wt-S2. The apoptosis induction indexes of JFH-1/S2-wt–transfected and JFH-1/wt-S2–transfected cells were 1.42 ± 0.13 and 1.71 ± 0.08, respectively (Fig. 5). These data indicate that both structural and nonstructural regions of JFH-1/S2 were associated with lower susceptibility to cytokine-induced apoptosis, although mutations in core-NS2 seemed to have higher contribution toward this phenotype. Together, these results indicate that the JFH-1/S2 strain, which was selected after passage in

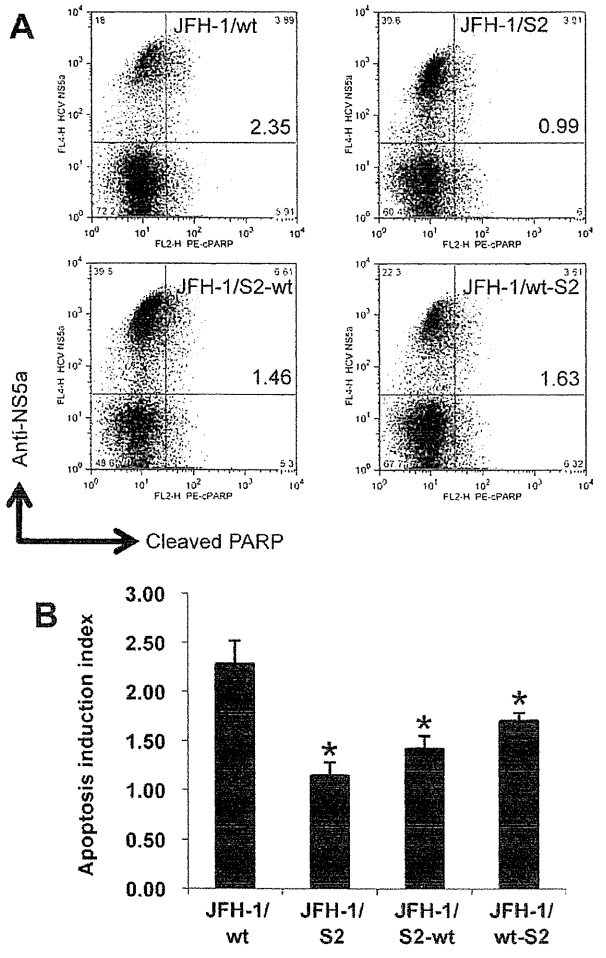

Fig. 5. Apoptosis induction in Huh-7.5.1 cells transfected with JFH-1/wt, JFH-1/S2, and their chimeric constructs. (A) Three million cells were transfected with 3 μg *in vitro*-transcribed full-genome RNA of JFH-1/wt, JFH-1/S2, JFH-1/S2-wt, and JFH-1/wt-S2. Apoptosis was induced by exposing cells to 20 ng/mL TNF-α plus 50 ng/mL actinomycin D and detected by anticleaved PARP staining. The clone names and apoptosis induction indexes are indicated in the upper right box. (B) Apoptosis induction indexes of JFH-1/wt-, JFH-1/S2-, JFH-1/S2-wt-, and JFH-1/wt-S2-transfected cells. The mean ± SD of three independent experiments is shown. *$P < 0.05$ versus JFH-1/wt.

the patient serum–infected chimpanzee, acquired less susceptibility to the cytokine-induced apoptosis.

Discussion

HCV develops chronic infection in the vast majority of infected patients[1]; however, the mechanisms of its persistence are still under investigation. Many viruses have evolved different strategies to cope with host immune systems, thus causing the development of persistent infection. For example, some viruses interfere with the major histocompatibility complex class I presentation of viral antigens, whereas others modulate lymphocyte and macrophage functions, including cytokine production.[12-16] In our previous study, we detected an increasing number of mutations in the HCV genome isolated from JFH-1 patient serum–infected chimpanzees. Thus, we reasoned that these detected mutations might have imparted some advantage to this virus for long-time survival. To examine this hypothesis, we compared the phenotypes of JFH-1 variant strains emerged at early and late stages of infection in JFH-1 patient serum–infected and JFH-1cc–infected chimpanzees and found that the JFH-1/S2 strain isolated from the patient serum–infected chimpanzee at a later time point of infection replicated slowly, produced more infectious viruses, and displayed reduced susceptibility to cytokine-induced apoptosis.

The JFH-1 variant strain JFH-1/C, which contains seven nonsynonymous mutations identified in the JFH-1cc–infected chimpanzee at week 7, showed comparatively slower replication kinetics and slightly enhanced infectious virus production in cell culture. The intracellular specific infectivity of this strain in Huh7-25 cells was 3.9 times higher than that of JFH-1/wt (Table 1). These characteristics might have imparted some advantage to this strain for establishing productive infection in the chimpanzee. The other JFH-1 variant strains, JFH-1/S1 and JFH-1/S2, contain 6 and 17 nonsynonymous mutations identified in the JFH-1 patient serum–infected chimpanzee at weeks 2 and 23 postinfection, respectively. Replication kinetics and infectious virus production of the JFH-1/S1 strain were comparable to that of JFH-1/wt in cultured cells (Fig. 1, Table 1). In contrast, the JFH-1/S2 strain showed lower replication efficiency. Although the intracellular HCV RNA level of this strain in Huh7-25 cells was lower than that of JFH-1/wt and JFH-1/S1, and almost the same as that of JFH-1/C (Table 1), intracellular specific infectivity was 18.0 and 12.9 times higher than that of JFH-1/wt and JFH-1/S1, respectively, suggesting a significant increase in the assembly of infectious virus particles ($P < 0.005$, Table 1). The enhanced capacity of this strain to assemble infectious virus particles resulted in a higher extracellular infectivity titer that contributed to the rapid spread of virus to surrounding cells. Flow cytometry analyses of cells transfected with JFH-1/wt and variant strains revealed that the percentage of the HCV NS5A-positive population in JFH-1/S2–transfected cells was higher, but the mean fluorescence intensity of the anti-NS5A signal was lower than that in JFH-1/wt–transfected cells, thus confirming higher spread and lower replication of this strain. Taken together, both JFH-1/C and JFH-1/S2 exhibited a tendency toward

decreased replication and increased infectious virus production. However, the extent of enhanced virus production was substantially lower in JFH-1/C than in JFH-1/S2, which might have led to the earlier elimination of infection in the JFH-1cc–infected chimpanzee. In other words, the potency of infectious virus production and spread seems to correspond to the duration of infection in infected animals.

The association between a lower replication efficiency and persistent infection is still unclear. It has been reported that an escape mutant with an amino acid substitution at the cytotoxic T lymphocyte (CTL) epitope in the NS3 region exhibits lower NS3/4 protease activity and replication capacity *in vitro*.[17,18] The JFH-1/S2 strain contains the T1077A mutation in the NS3 region (Supporting Table 1), and this mutation is located close to mutations reported to be associated with immune evasion and lower replication.[17] Thus, the lower replication efficiency of the JFH-1/S2 strain may be a result of an immune escape mutation at the expense of viral fitness. Meanwhile, we cannot deny the advantage of lower replication in establishing persistent infection. Lower replication may contribute to the avoidance of major histocompatibility class I–mediated antigen presentation and to escape from the host immune system. Either way, by acquiring the ability to produce more viral particles, the JFH-1/S2 strain could rapidly spread to surrounding cells, irrespective of its lower replication efficiency. Importantly, these emerged mutations did not attenuate *in vivo* infectivity, unlike cell culture adaptive mutations reported to cause attenuated infection *in vivo*.[19] Upon inoculation into human hepatocyte–transplanted mice, JFH-1/S1, JFH-1/S2, and JFH-1/C strains could establish infection without any mutations, produced levels of viremia similar to JFH-1/wt, and persisted for a similar observed period of infection (Fig. 2). This observation is different from that in chimpanzees, where JFH-1/wt and JFH-1/C strains were eliminated earlier than JFH-1/S2. In contrast to chimpanzees, human hepatocyte–transplanted mice lack a CTL and natural killer (NK) cell–mediated immune system, which could be responsible for this difference.[6] Taken together, our results suggest that along with efficient infectious virus production, the JFH-1/S2 strain might have acquired an advantage that helps it evade the CTL and NK cell–mediated immune system.

Apoptosis of virus-infected cells by the immune system is crucial as a general mechanism of clearing infections.[20,21] The J6/JFH-1 chimeric virus has been reported to exhibit proapoptotic characteristics in cell culture.[22] However, because HCV needs to escape the host immune system in order to establish chronic infection, immune cell–mediated apoptosis may be inhibited in infected hepatocytes. In the liver, HCV-infected hepatocytes are eliminated by targeted apoptosis induced by NK cells, macrophages, and CTLs with ligand-mediated and receptor-mediated signals such as TNF-α, FasL, and TNF-related apoptosis–inducing ligand.[23-26] Thus, we used TNF-α to mimic natural immunomediated apoptosis and found that the JFH-1/S2–replicating cells have lower susceptibility to the apoptosis induced by these cytokines. In JFH-1/S2–transfected cells, TNF-α–induced apoptosis detected by TUNEL assay was substantially lower than that of JFH-1/wt–transfected cells (Fig. 4). We confirmed it by staining with anticleaved PARP. In complete agreement with the results produced by way of TUNEL assay, the number of anticleaved PARP stained cells among JFH-1/S2–infected cells was significantly lower than that among JFH-1/wt–infected cells (Fig. 5). In our previous study, we reported that HCV-specific immune responses with T cell proliferation and interferon-γ production were maintained until the disappearance of viremia in the patient serum–infected chimpanzee.[11] This finding indicates that continuous selection pressure in the infected chimpanzee might have contributed to the emergence of a clone with an ability to escape the cytokine-induced apoptosis. We are not sure whether this phenotype of JFH-1/S2 is due to its lower replication efficiency and thus lower production of HCV proteins. The accumulation of viral proteins might predispose cells to the apoptosis induced by TNF-α. To answer this question, it will be necessary to investigate the genomic regions of JFH-1/S2 and cellular host factors responsible for the ability of this strain to escape the apoptosis.

By way of mapping analysis for JFH-1/S2, we could determine responsible regions; NS5B was for lower replication efficiency (Supporting Fig. 1B), and P7 and NS2 were for enhanced viral particle assembly (Supporting Table 2). For the evasion of apoptosis, we could not specify the responsible region, because both chimeric constructs, JFH-1/S2-wt and JFH-1/wt-S2, showed less susceptibility to cytokine-induced apoptosis to a certain extent. These data indicate that both structural and nonstructural regions might have contributed to the acquisition of this phenotype. Previously, a potent antiapoptotic effect of the HCV NS5A protein was described.[27] NS5A interacts with Bin1, which is a nucleocytoplasmic c-Myc–interacting protein with tumor suppressor and apoptotic properties, thus inhibiting Bin1-

associated apoptosis. Because JFH-1/S2 contains several mutations in the NS5A region (Supporting Table 1), one or more mutations in this protein may be associated with antiapoptotic effects.

In conclusion, we demonstrated that the JHF-1/S2 strain acquired phenotypes of lower replication, higher virus production, and less susceptibility to cytokine-induced apoptosis. These phenotypes were associated with mutations that emerged 23 weeks after infection in a chimpanzee, and might have contributed to long-term infection *in vivo*. Such control of viral functions by specific mutations may be a key viral strategy to establish persistent infection.

Acknowledgment: We are grateful to Francis V. Chisari for providing the Huh-7.5.1 cell line and Nao Sugiyama for technical assistance.

References

1. Liang TJ, Rehermann B, Seeff LB, Hoofnagle JH. Pathogenesis, natural history, treatment, and prevention of hepatitis C. Ann Intern Med 2000;132:296-305.
2. Feld JJ, Liang TJ. Hepatitis C—identifying patients with progressive liver injury. HEPATOLOGY 2006;43:S194-S206.
3. Thimme R, Oldach D, Chang KM, Steiger C, Ray SC, Chisari FV. Determinants of viral clearance and persistence during acute hepatitis C virus infection. J Exp Med 2001;194:1395-1406.
4. Thimme R, Bukh J, Spangenberg HC, Wieland S, Pemberton J, Steiger C, et al. Viral and immunological determinants of hepatitis C virus clearance, persistence, and disease. Proc Natl Acad Sci U S A 2002;99:15661-15668.
5. Mercer DF, Schiller DE, Elliott JF, Douglas DN, Hao C, Rinfret A, et al. Hepatitis C virus replication in mice with chimeric human livers. Nat Med 2001;7:927-933.
6. Tateno C, Yoshizane Y, Saito N, Kataoka M, Utoh R, Yamasaki C, et al. Near completely humanized liver in mice shows human-type metabolic responses to drugs. Am J Pathol 2004;165:901-912.
7. Kato T, Furusaka A, Miyamoto M, Date T, Yasui K, Hiramoto J, et al. Sequence analysis of hepatitis C virus isolated from a fulminant hepatitis patient. J Med Virol 2001;64:334-339.
8. Wakita T, Pietschmann T, Kato T, Date T, Miyamoto M, Zhao Z, et al. Production of infectious hepatitis C virus in tissue culture from a cloned viral genome. Nat Med 2005;11:791-796.
9. Zhong J, Gastaminza P, Cheng G, Kapadia S, Kato T, Burton DR, et al. Robust hepatitis C virus infection in vitro. Proc Natl Acad Sci U S A 2005;102:9294-9299.
10. Lindenbach BD, Evans MJ, Syder AJ, Wolk B, Tellinghuisen TL, Liu CC, et al. Complete replication of hepatitis C virus in cell culture. Science 2005;309:623-626.
11. Kato T, Choi Y, Elmowalid G, Sapp RK, Barth H, Furusaka A, et al. Hepatitis C virus JFH-1 strain infection in chimpanzees is associated with low pathogenicity and emergence of an adaptive mutation. HEPATOLOGY 2008;48:732-740.
12. Johannessen I, Crawford DH. In vivo models for Epstein-Barr virus (EBV)-associated B cell lymphoproliferative disease (BLPD). Rev Med Virol 1999;9:263-277.
13. Oglesbee MJ, Pratt M, Carsillo T. Role for heat shock proteins in the immune response to measles virus infection. Viral Immunol 2002;15:399-416.
14. Stevenson PG, Boname JM, de Lima B, Efstathiou S. A battle for survival: immune control and immune evasion in murine gamma-herpesvirus-68 infection. Microbes Infect 2002;4:1177-1182.
15. Alcami A. Viral mimicry of cytokines, chemokines and their receptors. Nat Rev Immunol 2003;3:36-50.
16. Wilkinson GW, Tomasec P, Stanton RJ, Armstrong M, Prod'homme V, Aicheler R, et al. Modulation of natural killer cells by human cytomegalovirus. J Clin Virol 2008;41:206-212.
17. Soderholm J, Ahlen G, Kaul A, Frelin L, Alheim M, Barnfield C, et al. Relation between viral fitness and immune escape within the hepatitis C virus protease. Gut 2006;55:266-274.
18. Uebelhoer L, Han JH, Callendret B, Mateu G, Shoukry NH, Hanson HL, et al. Stable cytotoxic T cell escape mutation in hepatitis C virus is linked to maintenance of viral fitness. PLoS Pathog 2008;4:e1000143.
19. Bukh J, Pietschmann T, Lohmann V, Krieger N, Faulk K, Engle RE, et al. Mutations that permit efficient replication of hepatitis C virus RNA in Huh-7 cells prevent productive replication in chimpanzees. Proc Natl Acad Sci U S A 2002;99:14416-14421.
20. Kagi D, Seiler P, Pavlovic J, Ledermann B, Burki K, Zinkernagel RM, et al. The roles of perforin- and Fas-dependent cytotoxicity in protection against cytopathic and noncytopathic viruses. Eur J Immunol 1995;25:3256-3262.
21. Kagi D, Vignaux F, Ledermann B, Burki K, Depraetere V, Nagata S, et al. Fas and perforin pathways as major mechanisms of T cell-mediated cytotoxicity. Science 1994;265:528-530.
22. Deng L, Adachi T, Kitayama K, Bungyoku Y, Kitazawa S, Ishido S, et al. Hepatitis C virus infection induces apoptosis through a Bax-triggered, mitochondrion-mediated, caspase 3-dependent pathway. J Virol 2008;82:10375-10385.
23. Kafrouni MI, Brown GR, Thiele DL. Virally infected hepatocytes are resistant to perforin-dependent CTL effector mechanisms. J Immunol 2001;167:1566-1574.
24. Guicciardi ME, Gores GJ. Apoptosis: a mechanism of acute and chronic liver injury. Gut 2005;54:1024-1033.
25. Fischer R, Baumert T, Blum HE. Hepatitis C virus infection and apoptosis. World J Gastroenterol 2007;13:4865-4872.
26. Stegmann KA, Bjorkstrom NK, Veber H, Ciesek S, Riese P, Wiegand J, et al. Interferon-alpha-induced TRAIL on natural killer cells is associated with control of hepatitis C virus infection. Gastroenterology 2010;138:1885-1897.
27. Nanda SK, Herion D, Liang TJ. The SH3 binding motif of HCV NS5A protein interacts with Bin1 and is important for apoptosis and infectivity. Gastroenterology 2006;130:794-809.

Research Article

EASL EUROPEAN ASSOCIATION FOR THE STUDY OF THE LIVER | JOURNAL OF HEPATOLOGY

Elimination of hepatitis C virus by short term NS3-4A and NS5B inhibitor combination therapy in human hepatocyte chimeric mice

Eiji Ohara[1,2], Nobuhiko Hiraga[1,2], Michio Imamura[1,2], Eiji Iwao[3], Naohiro Kamiya[3], Ichimaro Yamada[3], Tomohiko Kono[1,2], Mayu Onishi[1,2], Daizaburo Hirata[1,2], Fukiko Mitsui[1,2], Tomokazu Kawaoka[1,2], Masataka Tsuge[1,2], Shoichi Takahashi[1,2], Hiromi Abe[1,2], C. Nelson Hayes[2,4], Hidenori Ochi[2,4], Chise Tateno[2,5], Katsutoshi Yoshizato[2,5], Shinji Tanaka[1], Kazuaki Chayama[1,2,4,*]

[1]*Department of Medicine and Molecular Science, Division of Frontier Medical Science, Programs for Biomedical Research, Graduate School of Biomedical Sciences, Hiroshima University, Hiroshima, Japan;* [2]*Liver Research Project Center, Hiroshima University, Hiroshima, Japan;* [3]*Pharmacology Research Laboratories I, Mitsubishi Tanabe Pharma Corporation, Yokohama, Japan;* [4]*Laboratory for Digestive Diseases, Center for Genomic Medicine, RIKEN, Hiroshima, Japan;* [5]*PhoenixBio Co., Ltd., Higashihiroshima, Japan*

See Editorial, pages 848–850

Background & Aims: The current treatment regimen for chronic hepatitis C virus (HCV) infection is peg-interferon plus ribavirin combination therapy. The majority of developing therapeutic strategies also contain peg-interferon with or without ribavirin. However, interferon is expensive and sometimes intolerable for some patients because of severe side effects.

Methods: Using human hepatocyte chimeric mice, we examined whether a short term combination therapy with the HCV NS3-4A protease inhibitor telaprevir and the RNA polymerase inhibitor MK-0608 with or without interferon eradicates the HCV from infected mice. The effect of telaprevir and MK-0608 combination therapy was examined using subgenomic HCV replicon cells.

Results: Combination therapy with the two drugs enhanced inhibition of HCV replication compared with either drug alone. In *in vivo* experiments, early emergence of drug resistance was seen in mice treated with either telaprevir or MK-0608 alone. However, emergence was prevented by the combination of these drugs. Mice treated with a triple combination therapy of telaprevir, MK-0608, and interferon became negative for HCV RNA soon after commencement of the therapy, and HCV RNA was not detected in serum of these mice 12 weeks after cessation of the therapy. Furthermore, all mice treated with a high dose telaprevir and MK-0608 combination therapy for 4 weeks became negative for HCV RNA 1 week after the beginning of the therapy and remained negative after 18 weeks.

Conclusions: Eradication of HCV from mice with only 4 weeks of therapy without interferon points the way to future combination therapies for chronic hepatitis C patients.

Keywords: NS3-4A protease inhibitor; NS5B RNA polymerase inhibitor; Human hepatocyte chimeric mouse; Interferon.

Received 10 May 2010; received in revised form 14 July 2010; accepted 4 August 2010; available online 26 October 2010

DOI of original article: 10.1016/j.jhep.2010.09.034.

* Corresponding author at: Department of Medical and Molecular Science, Division of Frontier Medical Science, Programs for Biomedical Research, Graduate school of Biomedical Science, Hiroshima University, 1-2-3 Kasumi, Minami-ku, Hiroshima 734-8551, Japan. Tel.: +81 82 257 5190; fax: +81 82 255 6220.

E-mail address: chayama@hiroshima-u.ac.jp (K. Chayama).

Abbreviations: HCV, hepatitis C virus; IFN, interferon; RBV, ribavirin; SVR, sustained virological response; STAT-C, specifically targeted antiviral therapy for HCV; uPA, urokinase-type plasminogen activator; SCID, severe combined immunodeficiency; RT-PCR, reverse transcript-polymerase chain reaction; HSA, human serum albumin.

Introduction

Chronic hepatitis C virus (HCV) infection is a leading cause of cirrhosis, liver failure, and hepatocellular carcinoma [1,2]. The current standard treatment for patients chronically infected with HCV is the combination of peg-interferon (PEG-IFN) and ribavirin (RBV) [3–5]. However, this treatment results in a sustained viral response (SVR), defined as negative for HCV RNA 24 weeks after cessation of the therapy, in only about 50% of patients with genotype 1 HCV infection with high viral load [3–5]. In view of the lack of effectiveness of the current therapy, many molecules have been tested for development of novel anti-HCV therapies. Recently, a number of new selective inhibitors of HCV proteins, the so-called STAT-C (specifically targeted antiviral therapy for HCV) inhibitors, have been in development. The HCV NS3-4A protease inhibitor and the NS5B polymerase inhibitor, as well as an inhibitor of NS5A function, have been demonstrated to have potent anti-HCV effects and have proceeded to clinical trials [6].

Although the anti-viral effect of these drugs is quite potent, monotherapy using these drugs results in early emergence of drug-resistant strains [7,8]. Accordingly, these drugs are used in combination with PEG-IFN and RBV. However, because IFN-treatment is expensive and is frequently associated with serious adverse events, such as cytopenias, rash/itching, alopecia, and

mental disorders [3–5,9], a new treatment strategy, especially one that does not use IFN, is needed for chronic hepatitis C patients.

The immunodeficient urokinase-type plasminogen activator (uPA) mouse permits repopulation of the liver with human hepatocytes that can be infected with HCV [10]. We and other groups reported that the human hepatocyte chimeric mouse is useful for evaluating anti-HCV drugs such as IFN-alpha and the NS3-4A protease inhibitor [11–14]. In this study, we used the NS3-4A protease inhibitor telaprevir (VX950; MP424; Mitsubishi Tanabe Pharma Co., Osaka, Japan) [15] and the NS5B RNA polymerase inhibitor MK0608 (2′-C-methyl-7-deaza-adenosine) [16] and investigated the effect of a short term combination treatment with these drugs on HCV replication both *in vitro* and in *vivo*, and showed a successful elimination of viruses in HCV-infected chimeric mice without the use of IFN. Although the dose of the drugs used in this study might be intolerable in humans, elimination of the virus without IFN by only 4 weeks of therapy sheds light on approaches to developing combination therapies using multiple STAT-C agents without IFN.

Materials and methods

Cell culture

An HCV subgenomic replicon plasmid, pRep-Feo, was derived from pRep-Neo (originally, pHC-Vlbneo-delS [17]). The pRep-Feo carries a fusion gene comprising firefly luciferase (*Fluc*) and neomycine phosphotransferase, as described elsewhere [18,19]. Replicon RNA was synthesized *in vitro* by T7-RNA polymerase (Promega, Madison, WI) and transfected into Huh7 cells by electroporation. Huh7 cells were maintained in Dulbecco's modified Eagle medium (DMEM) containing 10% fetal bovine serum at 37 °C under 5% CO_2. After culturing in the presence of G418 (Wako, Osaka, Japan), cell lines stably expressing the replicons were established (Huh7/Rep-Neo).

Luciferase assay

Replicon cell lines were treated with various concentrations of either telaprevir or MK-0608 for 72 hrs, and HCV RNA replication level was quantified by internal luciferase assay. Luciferase activities were quantified using a luminometer (Lumat LB9501; Promega) and the Bright-Glo Luciferase Assay System (Promega). The 50% inhibitory concentrations (IC_{50}) were defined as the drug concentrations producing a 50% reduction in the levels of luciferase activities relative to average levels in untreated cultures.

MTT assays

Cell viability was measured under the same experimental settings using a tetrazolium (MTT)-based viability assay (BioAssay, California, USA) according to the manufacturer's directions. The 50% cytotoxic concentrations (CC_{50}) were defined as the drug concentrations producing a 50% reduction in absorbance relative to the average level in untreated cultures.

Animal treatment

Generation of the $uPA^{+/+}/SCID^{+/+}$ mice and transplantation of human hepatocytes were performed as described recently by our group [20]. All mice were transplanted with frozen human hepatocytes obtained from the same donor. All animal protocols described in this study were performed in accordance with the guidelines of the local committee for animal experiments, and all animals received humane care. Infection, extraction of serum samples, and sacrifice were performed under ether anesthesia. Mouse serum concentrations of human serum albumin (HSA), correlated with the repopulation index [20], were measured as previously described [21]. Eight weeks after hepatocyte transplantation, mice were intravenously injected with 100 μl of HCV-positive human serum samples. Mice serum samples were obtained every one or 2 weeks after HCV infection, and HSA and HCV RNA levels were measured.

Treatment with anti-HCV drugs in HCV-infected mice

Telaprevir and MK-0608 were dissolved with a specific solvent. Eight weeks after HCV infection when the mice developed stable viremia (10^6 to 10^9 copies/ml), mice were administered either 200 mg/kg of telaprevir or 3–50 mg/kg of MK-0608 orally twice a day for 4 weeks. The specific solvent had no anti-HCV effect in this mouse model (data not shown). To analyze the effect of the combination treatment with telaprevir and MK-0608, these drugs were mixed and given together as a cocktail. Human IFN-alpha-treatment was provided daily by intramuscular injection of diluted IFN solution (Otsuka Pharmaceutical Co., Ltd., Tokyo, Japan) for 4 weeks.

Human serum sample

Human serum containing a high titer of genotype 1b HCV (2.2×10^6 copies/ml) was obtained from a patient with chronic hepatitis who had provided written informed consent to participate in the study. Serum samples were divided into small aliquots and stored in liquid nitrogen until use. The study protocol conforms to the ethical guidelines of the 1975 Declaration of Helsinki and was approved by the institutional review committee.

RNA extraction and amplification

RNA extraction, nested PCR and quantitation of HCV by real-time polymerase chain reaction (PCR) were performed as described previously [12,13]. Briefly, RNA was extracted from serum samples and extracted livers using SepaGene RVR (Sankojunyaku, Tokyo, Japan) and reverse transcribed with a random hexamer and a reverse transcriptase (ReverTraAce; TOYOBO, Osaka, Japan) according to the instructions provided by the manufacturer. Quantitation of HCV cDNA was performed using Light Cycler (Roche Diagnostic, Japan, Tokyo). The lower detection limit of real-time PCR is 10^3 copies/ml.

Sequence analysis

The nucleotide and amino acid sequences of the NS3 and NS5B region of HCV were determined by direct sequencing following PCR amplification of cDNA after reverse transcription of HCV RNA. The primers used to amplify the NS3 region were 5′-GTGCTCCAAGCTGGCATAAC-3′ and 5′-AGGACCGAGGAATCGAACAT-3′ as the first (outer) primer pair and 5′-CTAGAGTGCCGTACTTCGTG-3′ and 5′-ACTGATCCTGGAGGCGTAGC-3′ as the second (inner) primer pair. The primers used to amplify the NS5B region were 5′-TAAGCGAGGAGGCTGGTGAG-3′ and 5′-CCTATTGGCCTGGAGTGTTT-3′ as the first (outer) primer pair and 5′-GACTCAACGGTCACTGAGAG-3′ and 5′-CCTATTGGCCTGGAGTGTTT-3′ as the second (inner) primer pair. PCR was performed in a 25 μl solution, consisting of a reaction buffer (12.5 μl, 2× PCR buffer for FOD FX), 5 μl 2 mM dNTPs, 0.75 μl F primer (10 μM), 0.75 μl R primer (10 μM), 1 μl Temp DNA (10 pg–200 ng), 0.5 μl KOD FX, 4.5 μl D.W. RT-PCR reactions were carried out following the manufacturer's instructions (Biometra T-Personal; Montreal Biotech Inc., Kirkland, QC, Canada). Amplification conditions included an initial denaturation at 94 °C for 2 min, 35 cycles of amplification (denaturation at 94 °C for 2 min, annealing of primer at 56 °C (1st PCR) or 59 °C (2nd PCR) for 30 s; extension at 68 °C for 2 min 30 s (NS3, 1st PCR), 1 min 30 s (NS3, 2nd PCR), 2 min (NS5B, 1st PCR), or 1 min 10 s (NS5B, 2nd PCR)); and final extension at 68 °C for 5 min.

Results

Anti-viral activity of telaprevir and MK-0608 on HCV subgenomic replicon cells

The effect of telaprevir and MK-0608 on HCV replication was analyzed *in vitro* using HCV replicon cells. Huh7/Rep-Feo cells were treated with various concentrations of either telaprevir or MK-0608. Measured luciferase activity demonstrated that both drugs inhibited HCV replication in a dose-dependent manner (Fig. 1). The IC_{50} of telaprevir and MK-0608 was 0.53 and 0.51 μM, respectively, consistent with previous reports [7,16]. When